ABSTRACT

Title of Dissertation / Thesis: MAPPING OF METAL ION BINDING SITES IN THE RECBCD ENZYME AND THE ROLE OF MAGNESIUM IN THE SUBUNIT INTERACTIONS OF RECBCD

Shamali Roy Choudhury, Doctor of Philosophy, 2006

Dissertation / Thesis Directed By: Prof. Douglas A. Julin

E. coli RecBCD is a 330kDa enzyme with three subunits RecB, RecC and RecD. The biological functions of RecBCD are to degrade foreign linear DNA and provide single stranded DNA to initiate homologous recombination. The enzyme has nuclease, helicase and ATPase activities. Divalent metal ions like Mg^{2+} are required for the nuclease and helicase activity of RecBCD. Previous work done by Dixon et al. (Dixon, D. A., Churchill, J. J., and Kowalczykowski, S. C. (1994) *Proc. Natl. Acad. Sci. USA* **91**, 2980-2984) and Taylor and Smith (Taylor, A. F., and Smith, G. R. (1999) *Genes & Devel.* **13**, 890-900) has shown that Mg^{2+} plays an important role in the interactions of the subunits and the activities of RecBCD. Identification of metal binding sites and the role of Mg^{2+} in the interaction of the subunits will enhance our understanding of the catalytic mechanism and structure of *E. coli* RecBCD.

The RecB subunit contains the 30kDa nuclease domain of RecBCD. Sequence comparisons have shown that the nuclease active site of the 30kDa nuclease domain is very similar to that of restriction endonucleases. Fenton chemistry techniques have

been used to map the metal binding sites of several restriction enzymes. We used Fenton chemistry techniques coupled with Edman sequencing to map the Mg^{2+} metal binding site of the 30kDa nuclease domain. A specific amino acid residue, Asp 1067 was identified as the metal binding site. Further corroboration that Asp 1067 was a unique Mg^{2+} binding site was obtained by doing mutational studies. Studies were also carried out in presence of other metals like Ca^{2+} to understand the details of the metal binding site.

The interactions between the RecB and RecC subunits of RecBCD are dependent on the presence of Mg^{2+} and DNA. We studied the role of magnesium on the binding interactions using surface plasmon resonance (Biacore) and found that Mg^{2+} enhances the binding interactions between the RecB and RecC subunits. Also, the role of magnesium in the binding of the RecC and 100kDa helicase domain of RecC were studied using ssDNA agarose chromatography, spin columns and gel filtration. Since, the 100kDa helicase domain requires Mg^{2+} for its helicase activity, we employed Fenton chemistry techniques coupled with mass-spectrometry to show that there is a metal binding site in the 100kDa helicase domain.

MAPPING OF METAL ION BINDING SITES IN THE RECBCD ENZYME AND THE ROLE OF MAGNESIUM IN THE SUBUNIT INTERACTIONS OF RECBCD

by

Shamali Roy Choudhury

Dissertation submitted to the Faculty of the Graduate School of the
University of Maryland, College Park, in partial fulfillment
of the requirements for the degree of
Doctor of Philosophy
2006

Advisory Committee:

Chair Prof. Douglas Julin, Dept. of Chemistry & Biochemistry, UMCP.
Prof. Dorothy Beckett, Dept. of Chemistry & Biochemistry, UMCP.
Prof. Steven Rokita, Dept. of Chemistry & Biochemistry, UMCP.
Prof. George Lorimer, Dept. of Chemistry & Biochemistry, UMCP.
Prof. Richard Stewart, Dept. of Cell Biol. & Mol. Genetics, UMCP.

Acknowledgements

I would like to thank Dr. Julin for giving me the opportunity to work with him. It has been a pleasure to work with him and have him as my mentor. His encouragement and in-depth knowledge of recombination helped me shape up exciting projects. I would also like to thank my committee members Dr. Beckett, Dr. Lorimer, Dr. Rokita and Dr. Stewart for their guidance and support. I would like to thank Dr. Beckett for her input on the visualization of small protein fragments using Tricine SDS PAGE. I would like to thank Dr. Rokita for his inputs on protein-metal interactions. I would like to thank Dr. Lorimer for his inputs on protein interactions. I would also like to thank Dr. Stewart for being my Dean's representative.

Thank you Dr. Peter Schuck, NIH for teaching me the operation of Biacore. I will also like to thank Dr. Brian Martin, NIH for sequencing my proteins.

I will like to thank all my lab members for their support. I will also like to thank the Department of Chemistry & Biochemistry for their continuous support. Thank you Emily, for being there for me during the ups and downs of my graduate study!

Table of Contents

List of Tables

List of Figures

List of Abbreviations

ATP	Adenosine triphosphate
C	Control
CV	Column volume
DTT	Dithiothreitol
dsDNA	double stranded DNA
E	Experiment
EDTA	Ethylenediamine tetraacetic acid
IPTG	Isopropyl-ß-D-thiogalactopyranoside
kDa	Kilodalton
M	Prestained Invitrogen Protein Marker
NBB	Native Binding Buffer
NEB	Native Elution Buffer
NTA	Nitrilotriacetic acid
NWB	Native Wash Buffer
PAGE	Polyacrylamide gel electrophoresis
PCR	Polymerase chain reaction
PMSF	Phenylmethylsulphonyfluoride
rpm	Rotations per minute
RT	Room Temperature
SDS	Sodium dodecyl sulfate
SSB	Single strand binding protein
ssDNA	Single stranded DNA

χ	Chi sequence

1 Chapter 1: Recombination and RecBCD

1.1 Introduction

From bacteria to mammals, recombination plays an important role in the repair of DNA damage induced by defects during replication. The site of these damages can either be the DNA itself or mutations in the replication enzymes. The event of recombination helps organisms to survive DNA damage and in the process gives rise to new genetic variants. Recombination can be either homologous or site specific. Homologous recombination has been well studied in *E. coli* and various mechanisms have been elucidated. One such mechanism uses the RecBCD enzyme.

RecBCD is a member of the Rec class of DNA-binding proteins from *E. coli* and is also known as Exonuclease V (1). RecBCD is a multimeric protein. It is composed of three different proteins called RecB, RecC and RecD. Each of these subunits has a defined activity. The function of the RecBCD enzyme in recombination is to generate single stranded DNA with the help of its nuclease and helicase activity. The single stranded DNA is then taken over by the SSB and RecA proteins to create stable intermediates, capable of undergoing recombination with homologous sections of the chromosome. The process of recombination is then completed by other enzymes like DNA polymerase, DNA ligase that repair the damaged portion of the DNA. RecBCD also has nuclease activity which helps E*. coli* to degrade viral DNA.(2)

There is evidence that the process of recombination, repair and replication may be intimately related. It was shown that mutants deficient in the PriA protein (functions in initiation at the replisome and recruitment of the replication enzymes) have a drastically reduced level of recombination dependent integration of conjugal DNA or P1 phage DNA into the chromosome (3).

1.2 Homologous Recombination

During meiosis the two homologous chromosomes are aligned next to each other and a cross-over takes place. Crossing over thus generates homologous recombination; that is, it occurs between two regions of DNA containing identical or nearly identical sequences. Usually, these are sequences on two equivalent regions of homologous chromosomes. At least in bacteria and yeast any two homologous DNA segments will recombine in the cell, given one condition: One of them must have a break or a region of single stranded DNA (4) A strong hint about the way crossing over begins is that breaks in the DNA greatly stimulate it. UV irradiation, X-ray irradiation and chemicals that create double-stranded breaks or gaps increase crossing over (5)**.** In *E. coli* several different gene products have been identified that play a role in the process of homologous recombination. The *rec* gene products play a central role in recombination with the help of other proteins including DNA polymerase, single strand binding protein (SSB), DNA topoisomerase, gyrase, ligase, and the RuvABC resolvasome (6). In 1965 the first *rec* gene was discovered (4). This was the *recA* gene and was identified by the isolation of recombination deficient mutants of *E. coli* K-12. These mutants could

conjugate with the donor DNA and receive the donor DNA but could not recombine that DNA with their own chromosomes. These mutants were also sensitive to UV radiation and it was shown that these mutants carried a single mutation that affected both recombination and UV resistance.

1.3 RecBCD Enzyme

Exonuclease V (RecBCD) was discovered as an ATP dependent DNase while studying DNA degradation with thermo-sensitive mutants of *E. coli*. Several other recombination deficient and UV sensitive mutants were identified simultaneously that lacked this enzyme (7). This enzyme is widely distributed in Gram-negative bacteria and has been most thoroughly studied in *E. coli.* The properties of *E. coli* RecBCD mutants lacking the enzyme reveal that the RecBCD enzyme is important for:

1.3.1 Homologous recombination

RecBCD is involved in homologous recombination events in *E. coli,* which includes conjugation, transduction and transformation. RecBCD catalyzed recombination events occur only in the presence of a DNA which is double-stranded and linear (2). This is called the Double Stranded Break Repair model (DSBR).

1.3.2 Recovery of DNA from damage and maintenance of cell viability

RecBCD in conjunction with RecA, DNA polymerase, and other enzymes repairs double-stranded breaks in DNA by a process of recombination repair.

1.3.3 Exclusion of foreign DNA

The nuclease activity of RecBCD is responsible for degrading foreign DNA. This activity is modulated by the Chi sequences to protect the *E. coli* genome from being degraded by the enzyme (8).

Double strand break repair model (DSBR):

This is the most general model for recombination and repair. It incorporates the various enzymes and the basic Holliday model. Double stranded breaks serve the paradoxical role of being both sites at which recombination initiates and lesions that are lethal. Hence, they are simultaneously loci that stimulate recombination and DNA damage that needs repair. The recombinational repair process consists of four steps.

Initiation: This is the first step in DSBR and represents the processing of the linear duplex DNA at the double stranded break to produce the ssDNA needed for DNA strand invasion of a dsDNA homologue by RecA. (For the prototypic homologous pairing reactions promoted by RecA protein ssDNA is a prerequisite) (6)

Homologous pairing and DNA strand exchange: The binding of RecA and SSB to the single stranded DNA leads to the formation of a presynaptic filament which then searches for a region of homology and initiates strand invasion

followed by base-pairing between the homologous regions. (A triple helix is probably formed). The resulting displacement of the recipient DNA strand leads to the formation of a D-loop. Base pairing of the invading strand of the donor DNA with the non-invading single strand of the recipient DNA results in the formation of a Holliday junction. Recombination specific helicases, the RecBCD and RecQ proteins work in conjunction with the RecJ exonuclease for the formation of the heteroduplex.

DNA heteroduplex extension: The extension takes place by branch migration. In this step a specialized motor protein complex, the RuvAB complex functions. The RuvAB complex is a DNA helicase that extends the region of the DNA heteroduplex by branch migrating over the cross over point (9).

Resolution: This is the final step of recombination. It requires the separation of the two conjoined DNA molecules. This is done by the Holliday junction specific RuvC endonuclease. The RuvC protein as a part of a complex with the RuvAB proteins recognizes and cleaves the Holliday junctions to complete the recombination process (10). The mechanism of homologous recombination and repair is shown below in Figure (1.1)

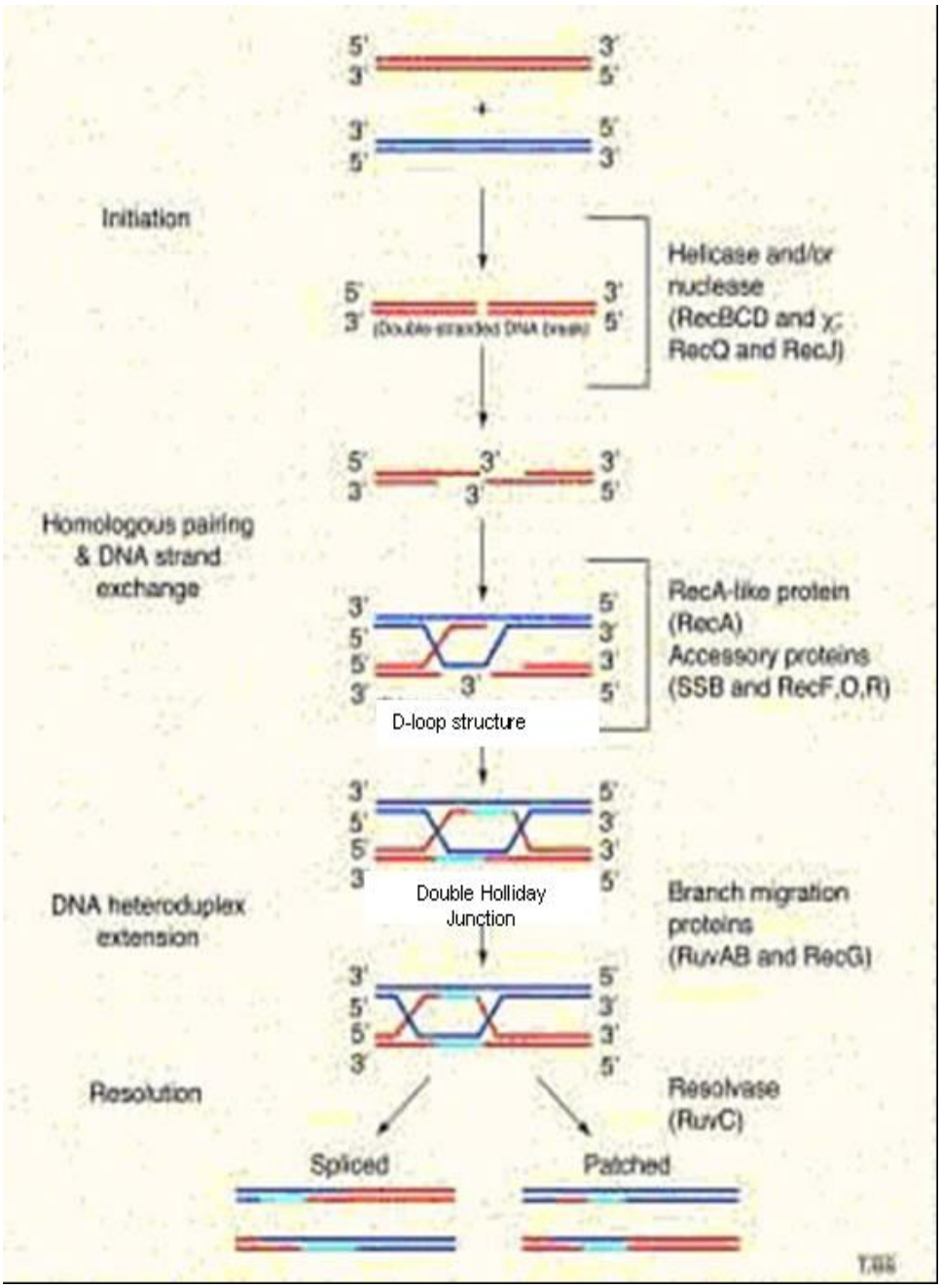

Figure 1.1: Double strand break repair model (6)

D-loop structure

1.4 The Subunits of RecBCD

RecBCD enzyme is a heterotrimer (11) of RecB (134kDa), RecC (129kDa) and RecD (67kDa). Genetic complementation analyses of ExoV null mutants revealed two genes, *recB* and *recC*, that coded for two polypeptides of mass 120 kDa and 110 kDa. These polypeptides were identified as RecB and RecC respectively.

The RecD protein was discovered after RecB and RecC. Purified preparations of ExoV can be dissociated by high salt and separated by column chromatography into two fractions, α and β (12). Mixing of α and β restores ATPase and nuclease activity. The β fraction contained the 120 kDa and 110 kDa polypeptides and the α fraction contained a 58 kDa polypeptide (1). The above molecular weights were obtained from an SDS PAGE gel. The composition of the α fraction was identified by using genetic complementation analysis of ExoV null mutants and recombination deficient mutants. Two mutants *recC*$^{-}$ and *recB*$^{-}$ belonging to a class of mutants designated as *recBC*$^{-}$ were studied. Unlike the recBC null mutants, the *RecBC*$^{-}$ are recombination proficient (but Chi nonactivating), resistant to DNA damaging agents and fully viable. Incubation of extracts from *recB*$^{-}$ mutant with the purified α fraction resulted in the appearance of ATP- dependent dsDNA exonuclease activity while incubation with β fraction produced no significant increase in this activity. Conversely, extracts of recC^{-} mutant produced ATP- dependent dsDNA exonuclease activity with the β fraction but not with the α fraction. The α fraction polypeptide was designated as RecD.

1.5 RecBCD: Genes and mutants

The three contributing genes of the RecBCD enzyme are closely grouped on the *E. coli* chromosome: *recB* and *recD* form an operon, while *recC* is situated nearby but has its own promoter (13). A combination of extremely weak promoters and suboptimal codons maintains the level of 10 RecBCD nuclease molecules per chromosome (14) None of its three genes are known to be SOS inducible. The physical map of the genes is shown below (Figure 1.2).

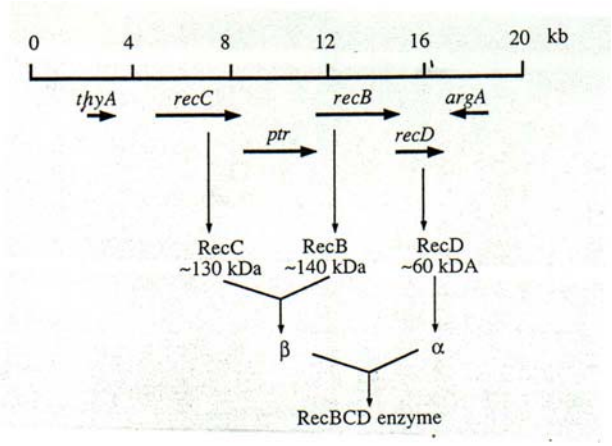

Figure 1.2: The RecBCD genes (15)

E. coli recB and *recC* null mutants are deficient in recombination following conjugation or generalized transduction. They are more sensitive than wild-type *E. coli* to DNA damaging agents such as X-rays, UV light, and mitomycin C (16). They are also sensitive to dsDNA phages (17).Cultures of *recBC* null mutants contain a large fraction of cells that fail to form visible colonies (18). This phenomenon called *lethal sectoring*, results in slower growth of *recBC* mutant colonies than the wild-type colonies. As a result the mutant colonies are reduced in size compared to the wild-type colonies.

In contrast null *recD* mutants and a single *recC* missense mutant display normal viability as well as wild-type survival after DNA damaging treatment (19). The *recD* mutants lack nuclease activity and are sensitive to dsDNA phages. They exhibit a $rec^{+}uv^{r}$ phenotype.

1.6 Biochemical Activities of RecBCD

RecBCD is a multimeric enzyme and was first discovered as an ATP dependent exonuclease (7). The prominent activities of RecBCD are as follows:

1. DNA dependent ATPase

2. ATP dependent nuclease (*ssDNA and dsDNA exonuclease and ssDNA endonuclease*)

3. ATP dependent helicase

4. Chi recognition activity

The Chi sequence (5'GCTGGTGG-3') inactivates the enzyme by attenuating its nuclease activity.

Each of these activities of RecBCD is needed for recombinational repair and has been localized to a particular domain of the enzyme complex.

1. DNA dependent ATPase and ATP dependent nuclease:

The nuclease activity of RecBCD requires ATP and proceeds at the same rate in the presence of a broad range of ATP concentrations. The requirement of ATP was demonstrated by isolation and characterization of an ATP dependent deoxyribonuclease encoded by the *recB* and *recC* genes (7). The extracts from wild type *E. coli* contained a DNase that catalyzed the release of acid soluble fragments from DNA. This activity was absent in *recB* and *recC* mutants. (The existence of the RecD subunit was still not known).

The two activities are linked to each other. The nuclease activity of RecBCD manifests itself only in the presence of both ATP and magnesium. RecBCD is unusual as a nuclease because DNA hydrolysis does not need an input of energy, and most nucleases do not hydrolyze ATP (20). RecBCD exhibits nuclease activity on circular or linear ssDNA and linear dsDNA. It functions as an exonuclease in both 3' to 5' and 5'to 3' orientations. DsDNA exonuclease is defined as the activity able to degrade linear duplex DNA RecBCD degrades linear duplex DNA to the same oligonucleotide products as are formed by ssDNA, but the degradation is faster and the rate of hydrolysis declines with increasing ATP concentrations (21). Circular duplex DNA, even containing single stranded nicks and short gaps are refractory to RecBCD attack (22) because the

enzyme can enter duplex DNA only through double-stranded ends (23). It can also act as an ssDNA endonuclease to cut and degrade circular ssDNA. RecBCD degrades ssDNA to fragments several nucleotides in length and these fragments are acid-soluble.

The degradation of duplex DNA by RecBCD requires both Mg^{2+} and ATP. The rate of degradation is dependent on the ratio of these two ions.(24) ATP and Mg^{2+} complex with each other, and so in an equimolar solution there is little free Mg^{2+} or ATP. The nuclease activity of RecBCD is stimulated when the Mg^{2+} concentration exceeds that of ATP and is inhibited when the ATP concentrations exceed that of Mg^{2+} (11).

2. ATP dependent helicase:

The third major activity of the RecBCD enzyme is DNA unwinding. RecBCD is a potent and highly processive DNA helicase (25). DNA unwinding by RecBCD requires ATP and magnesium. The explanation for the unusual ATP-dependent dsDNA exonuclease activity of RecBCD is that the enzyme is able to hydrolyze duplex DNA only after its unwinding. The helicase activity was measured using a novel assay. The assay takes advantage of the quenching of the intrinsic protein fluorescence of *E. coli* SSB protein upon binding to ssDNA. This is used to characterize the DNA unwinding activity of RecBCD enzyme. Unwinding in this assay is dependent on the presence of ATP, RecBCD enzyme, and linear dsDNA (25).

3. Chi-recognition activity:

One of the functions of the RecBCD enzyme is to degrade invading foreign DNA. At the same time this enzyme has to repair the double stranded break in the *E. coli* genome by recombinational repair. Several activities like the helicase and nuclease activities of RecBCD are regulated by an 8-nt symmetric DNA sequence χ (5′-GCTGGTGG-3′), which is recognized by the RecBCD enzyme. Chi sites are DNA sequence elements that stimulate the RecBCD enzyme dependent recombination in their vicinity. These are recombination hotspots. Genetic and physical analysis has determined that these recombination hotspots are composed of the sequence 5'-GCTGGTGG-3' (26). When RecBCD enzyme encounters χ, the intensity and polarity of its nuclease activity are changed, and the enzyme gains the ability to load RecA protein onto the χ-containing, unwound single-stranded DNA. The presence of the 8-nt Chi sequence in the *E. coli* genome prevents the degradation of the *E. coli* genome by interacting with RecBCD. RecBCD enzyme catalyzes Chi-dependent cleavage of one the DNA strands containing the Chi sequence, 5'-GCTGGTGG-3'. Stimulation of recombination by Chi occurs primarily to the 5' side of the Chi site and requires a functional RecBCD enzyme. Chi-specific cleavage is greatly reduced by single base pair changes within the Chi sequence and by mutations within the *E. coli* RecC gene (27).On approaching the Chi sequence the RecBCD enzyme nicks the DNA. *In vitro* recognition of Chi by RecBCD enzyme is

orientation dependent and results in a site specific nick in the DNA strand containing the Chi sequence 4-6 not to the 3' side of the Chi sequence (Figure 3, step a). RecBCD must approach the Chi site from the 3' side for a specific nick to occur (23). The 3′ terminal at the entry site of RecBCD enzyme is degraded much more vigorously than the 5′ terminal strand (28) After binding to a double-stranded DNA end, RecBCD hydrolyzes ATP to translocate and separate the duplex while preferentially degrading the 3'-terminated nascent single strand. The RecBCD enzyme requires only the sequence information in the 5'-GCTGGTGG-3'-containing strand to recognize and to be regulated by Chi. Furthermore, interaction with the recombination hotspot χ causes an attenuation of the nuclease activity but not of the helicase activity and is accompanied by a pause of RecBCD enzyme at the χ site (Figure 1.3, step b). Once the enzyme encounters Chi, the translocating enzyme pauses and subsequent cutting on the 3'-strand is attenuated leading to production of a Chi-specific DNA fragment, the length of which is equal to the length of the DNA from Chi to the 5' end of the strand (27,28).

This single strand is then taken over by RecA and homologous recombination occurs (Figure 1.3c). The ssDNA strand covered with RecA then invades the homologous dsDNA to produce a D-loop structure and initiate recombinational repair with the help of other enzymes (Figure 1.3d). In addition to the attenuation of the 3' to 5' nuclease activity a weaker 5' to 3' nuclease activity is activated in the 5' terminal strand. This switch in the polarity of nuclease activity produces a dsDNA molecule with an ssDNA tail retaining χ at the 3’ terminus (Figure 1.3e & 1.3f).

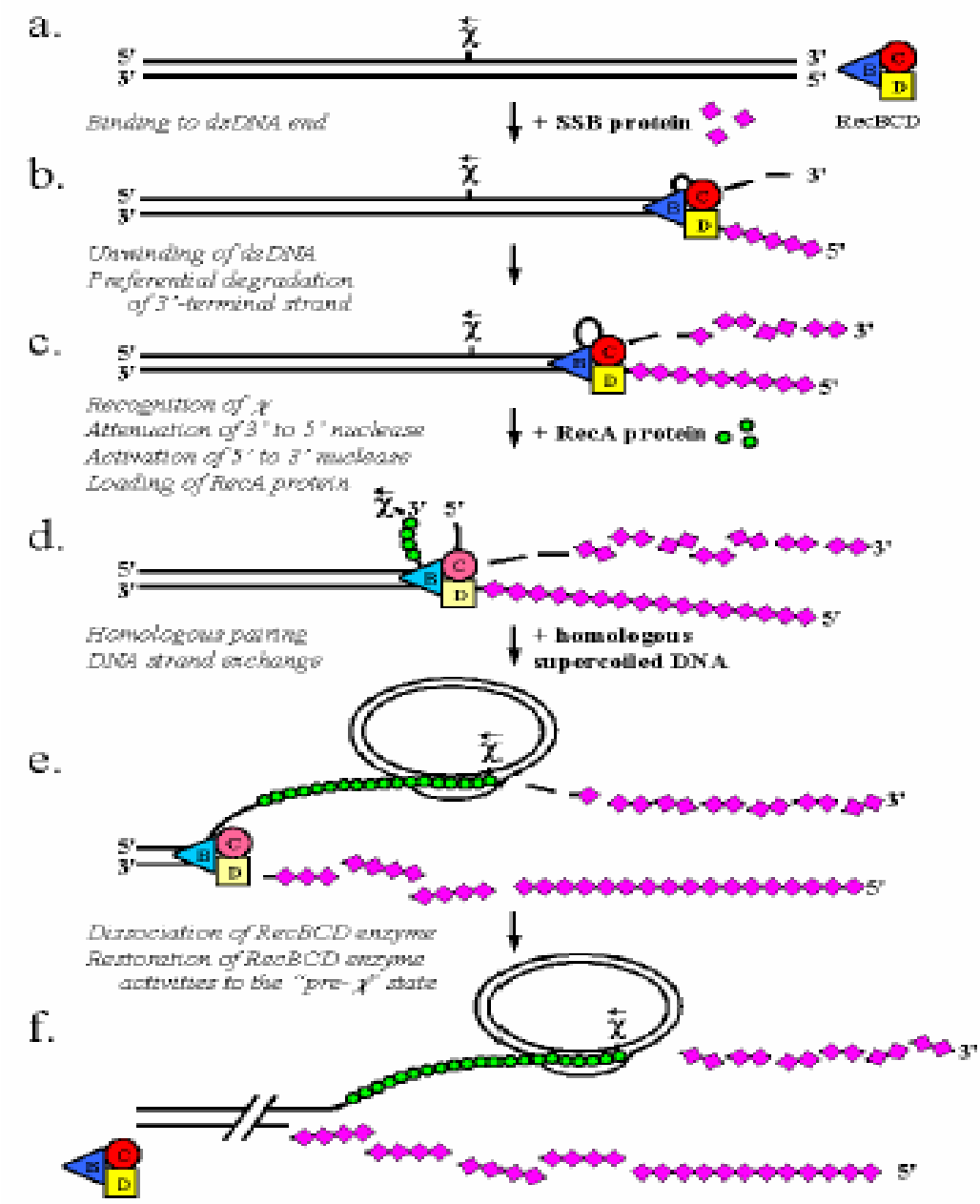

Figure 1.3: Initiation of recombination dependent DNA repair by RecBCD and RecA enzymes (2)

1.7 RecBCD: The role of RecB, RecC and RecD subunits

The RecBCD enzyme is comprised of three subunits arranged as a 330-kDa heterotrimer that is fully functional without the need for further oligomerization (12). The complex range of enzyme activities catalyzed by RecBCD can be attributed to the three subunits as follows: RecB is a 3'–5' helicase and multifunctional nuclease, RecC recognizes Chi, and RecD is a 5'–3' helicase.

Photo-affinity labeling of the RecBCD enzyme was done with 8-azidoadenosine 5'-triphosphate.The RecB and RecD subunits of the RecBCD enzyme (exonuclease V) from *E. coli* were covalently photo-labeled with the ATP photo affinity analogue [alpha-^{32}P] 8-azido-ATP. ATP strongly inhibited the photo labeling. 8-azido-ATP is hydrolyzed by the RecBCD enzyme and this supported its double-stranded DNA exonuclease activity. Also the label is largely confined to two peptides obtained by tryptic digestion of the photo labeled holoenzyme. One is derived from the RecB subunit and the other from the RecD subunit (29).

RecB and RecC:

RecB protein has been shown to exhibit DNA-dependent ATPase activity. The amino acid sequence of RecB and photo affinity labeling with 8-azidoadenosine 5'-triphosphate, an analogue of ATP showed that RecB had ATP binding sites. The purified RecB protein can also function as a DNA helicase. The RecB subunit could displace oligonucleotides annealed to viral M13 DNA in an

ATP dependent and orientation-specific manner (30). RecC protein alone has neither ATPase nor exonuclease activity. However, when combined together, the RecBC complex shows higher ATPase and helicase activity than RecB by itself (31). The RecBC complex is still a very weak nuclease (exonuclease and endonuclease). A class of recC mutants lacks Chi recognition activity. This suggests that probably the Chi recognition activity reside in the RecC polypeptide.

Limited proteolysis was carried out on the RecB subunit with subtilisin. Subtilisin cleavage of purified 130 kDa RecB gives rise to two fragments; a 100 kDa N-terminal domain (residues 1-929) and a 30 kDa C-terminal domain (32). With longer incubation time the 100 kDa fragment was degraded further whereas the 30 kDa fragment was resistant to further degradation. The 100 kDa and the 30 kDa fragments were separated using chromatographic separation with a ssDNA-agarose or heparin-agarose column. The 30 kDa fragment did not bind to these columns, whereas the 100 kDa bound to the column and had an elution pattern identical to intact RecB. This suggested that the 100 kDa fragment is responsible for binding to DNA. A linker region links the 100 kDa N-terminal and the 30 kDa C-terminal domains. A truncated RecB mutant was created ($RecB_{1-929}$) by deleting the DNA encoding the 251 amino acids from the C-terminal end. The truncated $RecB_{1-929}$ protein was over expressed and purified. The protein showed helicase activity by its ability to unwind linearized plasmid DNA. $RecB_{1-929}$ was able to unwind DNA and the processivity of unwinding increased in the presence of RecC. It was then reconstituted with RecC and His-tagged RecD. Helicase and nuclease assays were done with this protein. The $RecB_{1-929}$ CD did not show any

nuclease activity as manifested by its inability to cut any of the three substrates (linear ssDNA, circular ssDNA and linear dsDNA) of RecBCD. This suggested that the 30 kDa C-terminal domain is essential for nuclease activity of RecBCD.

The 30 kDa C-terminal domain was shown to have nuclease activity by the creation of a chimerical enzyme by attaching the 30 kDa C-terminal domain to the gene 32 protein of T4 phage. This chimera was created because the 30 kDa C-terminal domain did not bind the ssDNA agarose column. To identify the nuclease active site Asp427 in the 30kDa C-terminal domain chimerical enzyme (= Asp1080 in RecB) was substituted by Ala. This abolished all nuclease activity and indicated that there is a single nuclease active site in RecB, which is localized to the 30kDa region. This mutation did not affect the helicase activity (33).

RecD:

RecD has ATP binding sites and a weak ATPase (3). The addition of RecBC to RecD produces a potent dsDNA exonuclease. The nuclease activity of RecBC increases on the reconstitution of the holoenzyme (34). Although identified as a ssDNA-dependent ATPase several years ago (35) and shown to contain several characteristic helicase motifs20, it was only recently shown that the RecD subunit has 5'–3' helicase activity. (36) (37).

1.8 Crystal Structure of RecBCD

RecBCD is a bipolar helicase that splits the duplex into its component strands and digests them until encountering a recombinational hotspot (Chi site).

The nuclease activity is then attenuated and RecBCD loads RecA onto the 3' tail of the DNA. The crystal structure of RecBCD bound to a DNA substrate has been solved showing that the dsDNA strand is split into two across the RecC (38). Each of these single stranded DNA then align themselves toward two helicase motor subunits. The strands pass along tunnels within the enzyme, and emerge near the nuclease domain of RecB. The recognition of the Chi sequence occurs in this tunnel and this in turn regulates the nuclease activity. The crystal structure of the RecB nuclease domain also shows a calcium coordinated to the side chains of three residues (His 956, Asp 1067 and Asp 1080) and the main-chain carbonyl of Tyr 1081. It is likely that this calcium ion is bound at the position where a magnesium ion would normally bind in the active site of the protein, because calcium has been shown to be an inhibitor of the nuclease activity. (39)

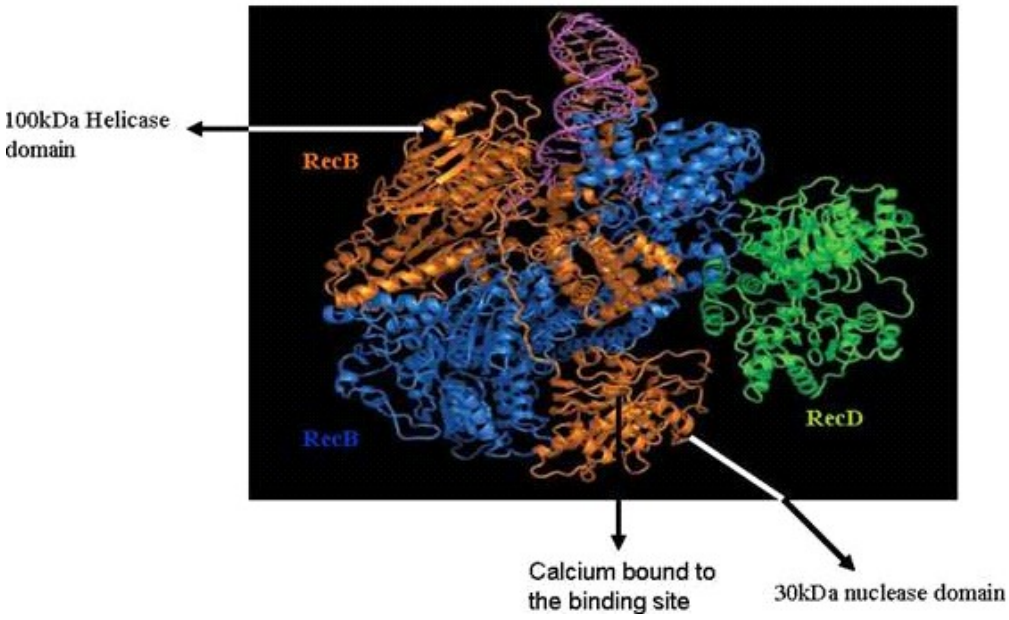

Figure 1.4: Crystal Structure of RecBCD (38)

1.9 Role of Magnesium

Divalent metal ions play a crucial role in forming the catalytic centers of various DNA nucleases. RecBCD requires both Mg^{2+} and ATP for its activity. Mg^{2+} is a divalent metal ion which is required for the nuclease and helicase activity and interactions of the RecBCD subunits as well. A single nuclease active site has been identified in the C-terminal 30kDa domain of the RecB subunit of the RecBCD holoenzyme (32). The nuclease activity of RecBCD is attenuated on encountering an octameric sequence called Chi (3'-GGTGGTCG-5'). Regulation at Chi depends strongly on the concentration of ATP and Mg^{2+}. The degradation of duplex DNA by RecBCD requires both Mg^{2+} and ATP. The rate of degradation is dependent on the ratio of these two ions. ATP and Mg^{2+} complex with each other, and so in an equimolar solution there is little free Mg^{2+} or ATP. The nuclease activity of RecBCD is stimulated when the Mg^{2+} concentration exceeds that of ATP and is inhibited when the ATP concentrations exceed that of Mg^{2+}.

The inactivation of RecBCD on encountering Chi was proposed to result from the complete disassembly of the enzyme to its individual subunits (40). Enzyme inactivation was studied in presence of tandem Chi sequences and low magnesium and high ATP concentration. Taylor and Smith analyzed the Chi inactivated enzyme disassembly by glycerol gradient ultracentrifugation and native gel electrophoresis. Ultracentrifugation showed that very little intact enzyme was left after it was treated with Chi containing DNA sequences. RecC sedimented as expected of the free polypeptide whereas RecB sedimented faster than free RecB but slower than the RecBC complex. Further, RecB did not co-

sediment with RecD. The faster sedimentation of RecB was explained by a RecB-DNA complex. The RecD sedimented as a trimeric species because it is very hydrophobic and forms aggregates. Taylor et al also corroborated their findings by observing the migration of the Chi inactivated RecBCD enzyme on a native gel.

Dixon et al showed that under conditions of limiting Mg^{2+} ion there is reversible inactivation of the enzyme; addition of excess Mg^{2+} reactivates all activities of the enzyme (24). They observed that RecBCD unwound only Chi containing DNA when the ATP concentration was higher than that of magnesium, resulting in low free magnesium concentrations. Under the conditions of limiting magnesium (less than 10mM) Dixon et al showed that dsDNA unwinding activity is inhibited. This inactivation is reversed when the concentration of magnesium is increased. To examine the inhibitory effect of Chi on dsDNA unwinding Dixon et al used fluorescence helicase assay and found that at limiting magnesium concentrations RecBCD unwound ds DNA till it encountered Chi. At Chi RecBCD pauses and becomes equivalent to RecBC and unwinding can be reinitiated by the addition of magnesium. Based on their studies they proposed a model in which the RecD subunit is ejected or functionally inactivated after RecBCD interacts with a Chi sequence.

The above observations suggest that there is some change in the subunit-subunit interaction at Chi. These changes were dependent on the concentration of Mg^{2+} and subunit disassembly. However, the exact nature of these changes was not known. We looked into the role of the divalent magnesium ion closely. In an

effort to understand the role of magnesium we studied the effect of magnesium on the binding of RecB and RecC proteins and then went on to map the magnesium metal binding sites in the RecB subunit.

Alignment of the C-terminal sequence of *E. coli* RecB with homologous proteins from other bacteria identified conserved aspartates at position 1067 and 1080 and a lysine at position 1082. Mutation of the amino acid residues Asp1080, Asp1067 and Lys1082 abolished nuclease activity on both single and double stranded DNA. Together with Asp1080, these residues compose a motif that is similar to one shown to form the active site of several restriction endonucleases (41). Mg^{2+} ion has been shown to play a role in the activity of nucleases containing acidic residues in their active site(42).

1.10 Fenton Chemistry

This process uses transition metals to catalytically oxidize chelating ligands with deleterious effects. More recently, Fenton chemistry techniques have been applied to investigate the active sites of proteins by using reagents which oxidatively cleave the polypeptide backbones of enzymes at their metal-binding sites (43-45). Fe^{2+} is most commonly used to cause oxidative cleavage of proteins (42,46). The metal-catalyzed oxidation generates reactive species ($O_2\cdot$ or OH) through Fenton Chemistry (43). The reactive species can interact with nearby susceptible amino acid residues can specifically cleave the polypeptide backbone in close proximity to the site where the reactive species are formed. A schematic representation is shown in Figure (1.5). The hydroxyl radical reacts with the

polypeptide backbone in the vicinity of the metal binding site. The hydroxyl radical abstracts the α hydrogen of the amino acid near the metal binding site and cleaves the peptide backbone generating peptide fragments. The purified enzyme was treated with Fe^{2+} and ascorbate. The ascorbate helps in maintaining the +2 oxidation state of Fe. The cleavage products from the protein after treatment with Fe^{2+} are sequenced using Edman degradation to identify the amino acid at the metal binding site.

In an attempt to identify the amino acids involved in metal binding at the active sites of endonucleases, Andersen et al, substituted Mg^{2+} ions by Fe^{2+} ions in two archaeal intron encoded homing endonucleases, I-*Dmo*I and I-*Por*I, yielding functional enzymes and enabling the generation of reactive hydroxyl radicals within the metal ion binding sites (47). Specific hydroxyl radical-induced cleavage was observed within, and immediately after, two conserved LAGLIDADG motifs in both proteins and at sites at, and near, the scissile phosphates of the corresponding DNA substrates. The dual protein/ nucleic acid foot printing approach implemented by Andersen et al, is generally applicable to other protein–nucleic acid complexes when the natural metal ion can be replaced by Fe^{2+}. Hlavaty et al, employed Fenton chemistry techniques to identify the residues involved in metal binding located at the active sites of restriction endonucleases. The restriction endonucleases *Bam*HI, *Fok*I, *Bgl*I, *Bgl*II, *Pvu*II, *Sfi*I, *Bss*SI, *Bso*BI, *Eco*RI, *Eco*RV, *Msp*I, and *Hin*P1I were subjected to oxidizing conditions in the presence of Fe^{2+} and ascorbate. All proteins were inactivated upon treatment with Fe^{2+} and ascorbate. *Bam*HI, *Fok*I, *Bgl*I, *Bgl*II, *P*vu*I*I, *Sfi*I,

*Bss*SI, and *Bso*BI were specifically cleaved upon treatment with Fe^{2+}/ascorbate. The site of Fe^{2+}/ascorbate induced protein cleavage for each enzyme was determined. The metal binding amino-acids found by the Fe-mediated cleavage reactions has also been shown by structural and mutational studies to be involved in both metal ligation and catalysis (42).

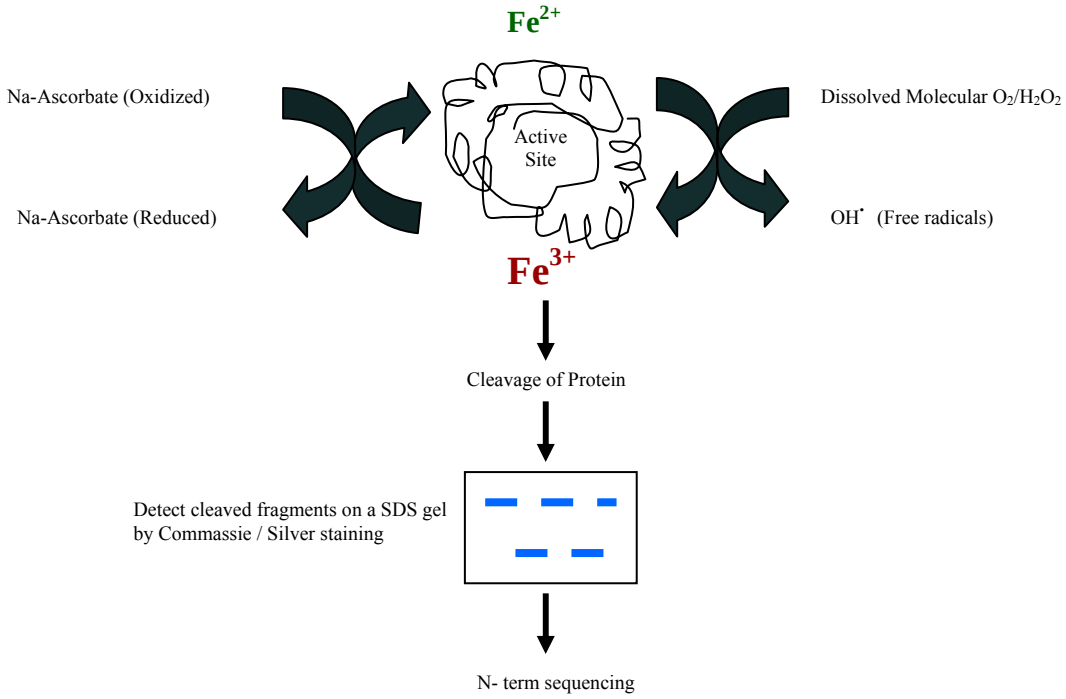

Figure 1.5: Schematic representation of Fe-cleavage of proteins.

RecBCD is a complex enzyme which has many functions; helicase, nuclease, ATPase. Each of these activities is carried out by one or more subunits of this protein. A lot of studies to date have explored the activities of this protein. In my thesis I have tried to study the structure-functional relationship of RecBCD using a variety of biochemical and biophysical techniques.

Divalent metal ions like Mg^{2+} are required for the nuclease activity of RecBCD. Identification of metal binding sites will enhance our understanding of the catalytic mechanism and structure of *E. coli* RecBCD. The C-terminal 30kDa domain of the RecB subunit contains the nuclease active site of RecBCD. We used Fenton chemistry techniques to identify the amino acid that binds the magnesium metal in the 30kDa domain.

The various activities of the *E. coli* RecBCD enzyme are very sensitive to reaction conditions. Inclusion of calcium in low concentrations affects dsDNA exonuclease and ssDNA exonuclease activities but the DNA dependent ATPase activity is not affected (39). This finding coupled with the crystal structure of RecBCD which showed a bound calcium in the nuclease active site indicates that calcium binds more strongly to the nuclease active site than magnesium. Hence, to corroborate our findings we carried out the Fe-cleavage reactions in presence of calcium.

Magnesium is also required for the interactions between the subunits of RecBCD and the for its helicase activity (24, 40). We used a variety of biophysical techniques like Biacore, ssDNA agarose chromatography, spin

columns and gel filtration to probe the role of magnesium in the interactions between the RecC and RecB subunits of RecBCD. Moreover, the N-terminal 100kDa domain of the RecB subunit contains the helicase activity of RecBCD. So, we also attempted to use Fenton chemistry techniques to identify the magnesium binding site in the helicase domain of RecBCD.

2 Chapter 2: Mapping of Metal Binding Sites in the Nuclease Domain of RecBCD

2.1 Introduction:

RecBCD enzyme is a DNA dependent ATPase and an ATP dependent helicase and exonuclease. RecBCD also requires Mg^{2+} ion for its ATPase, nuclease, and helicase activities. The single nuclease active site of RecBCD is located in the 30kDa domain of the RecB subunit of RecBCD. Metal binding sites in restriction enzymes have been mapped using Fenton chemistry techniques. We employed this method to map the magnesium metal binding site in the RecB nuclease domain. Different reaction conditions were tested to arrive at an optimal condition where the clear cleavage products were maximally formed and could be visualized.

A comparative study was done with the wild type 30kDa and two mutants where the aspartate residues at 1067 and 1080 were mutated to an alanine residue (D1067A mutant of the 30kDa and D1080A mutant of the 30kDa). These aspartate residues are crucial for nuclease activity of RecBCD (33). The aspartate residue has a negative charge and this helps in binding of the positively charged magnesium ion. The significance of the Asp1067 residue in metal binding was corroborated by constructing a mutant 30kDa in which the Asp residue at 1067 was mutated to an uncharged Ala residue. The effect of Fe-cleavage was also studied on the D1080A mutant which had an Asp residue at position 1080 mutated to Ala. This mutant was previously shown to have reduced nuclease

activity. The comparative study of the wild-type and the mutants corroborated that the Asp1067 residue of the 30kDa nuclease domain of RecB is the binding site of the magnesium metal ion.

2.2 Material and Methods

All protein and DNA molecular mass markers were from Invitrogen. The chemicals used for buffers used during protein purification were either from Sigma, Fisher or J.T. Baker. The *E. coli* strain used for the expression and purification of the 30 kDa RecB nuclease domain was BL-21. The plasmid containing the 30kDa sequence was pET 15b-30 (34) which has ampicillin resistance. Ampicillin was used at a concentration of (25 mg/ml) for the BL-21 strains carrying the pET 15b-30 plasmid. Culture media were LB broth (Fisher) and agar plates containing ampicillin. The BL-21 cells expressing the 30kDa protein were grown at 37 ºC with shaking at 250rpm.

2.2.1 Purification of the 30kDa subunit:

Each batch of purification was done using a culture volume of 2 - 10 liters. An overnight 50 ml seed culture was grown to saturation. This saturated culture was used to start the larger cultures the next day. The dilution was 1:200. The cells were induced with 1mM IPTG after the cells had reached log phase (OD_{650} = 0.5) and induction was carried out for 3-4 hrs. The cells were harvested using a JA 10 rotor in a Beckman centrifuge at 10,000 X g for 10 minutes. The pelleted

cells were stored at –80 °C. The cells were lysed the next day after re-suspending them in the first buffer that was used to load the column. Protease inhibitor cocktail (Sigma) was added to the resuspended cells before lysis. Cell lysis was done using a Branson 300 Sonicator at a duty cycle of 30% for 30 seconds for an average of 10-15 cycles. Care was taken so that frothing did not take place during cell lysis using sonication. The lysate was cleared by centrifuging the crude cell lysate at 20000 g using a JA 20 rotor for 90 minutes at 4 °C in a Beckman centrifuge. The lysate was then decanted into a polypropylene tube and filtered using a 0.22 micron syringe filter. It is important to filter the crude lysate before loading them on the FPLC columns to avoid clogging of the filters.

The purification of the 30kDa protein was done using 5 ml Hi-Trap chelating HP columns on an AKTA FPLC system from Amersham-Pharmacia. The column was charged using a 10mM $NiCl_2$ solution. The column and the super loop were then equilibrated with the Native Binding buffer (pH = 7.8) (see Table 2.1 for the composition). The filtered lysate was then injected into the loop using a syringe. The lysate was loaded on the column at a flow rate of 1-2 ml/min. The unbound protein was washed using 2 CV of the native binding buffer followed by Native Wash Buffer containing 60mM imidazole (pH=6.0) at a flow rate of 3 ml/min. The protein was eluted from the column by applying a gradient of 10 CV of 60mM - 1M imidazole at a flow rate of 1.5ml/min. The native binding, wash and elution buffers contained 20mM KPO_4 and 10mM NaCl. PMSF (100 mm) was added to the buffers just before the purification of the protein to prevent degradation. The fractions containing the eluted protein were pooled and dialyzed

against a buffer containing 20mM Tris and 50% glycerol (pH = 7.5) for storage at -80 °C. The elution profile of the 30 kDa protein is shown below (Figure 2.1). Column settings of the Akta FPLC for the purification of 30kDa are listed in Table (2.1). The program used to automate the process was written using Unicorn software provided by Amersham.

The protein starts to elute at 40% gradient and is completely eluted around 59% as shown in Figure (2.1). The fractions B11- B3 under the peak fraction elution peaks were checked on a 12% SDS gel. For this purpose 20µl of sample along with 5µl of 3.3X loading dye was loaded on the gel. The figure (2.2) shows that the 30kDa is present in the above fractions but large amounts of GroEL (molecular weight ~60 kDa) has co-purified with the 30kDa domain.

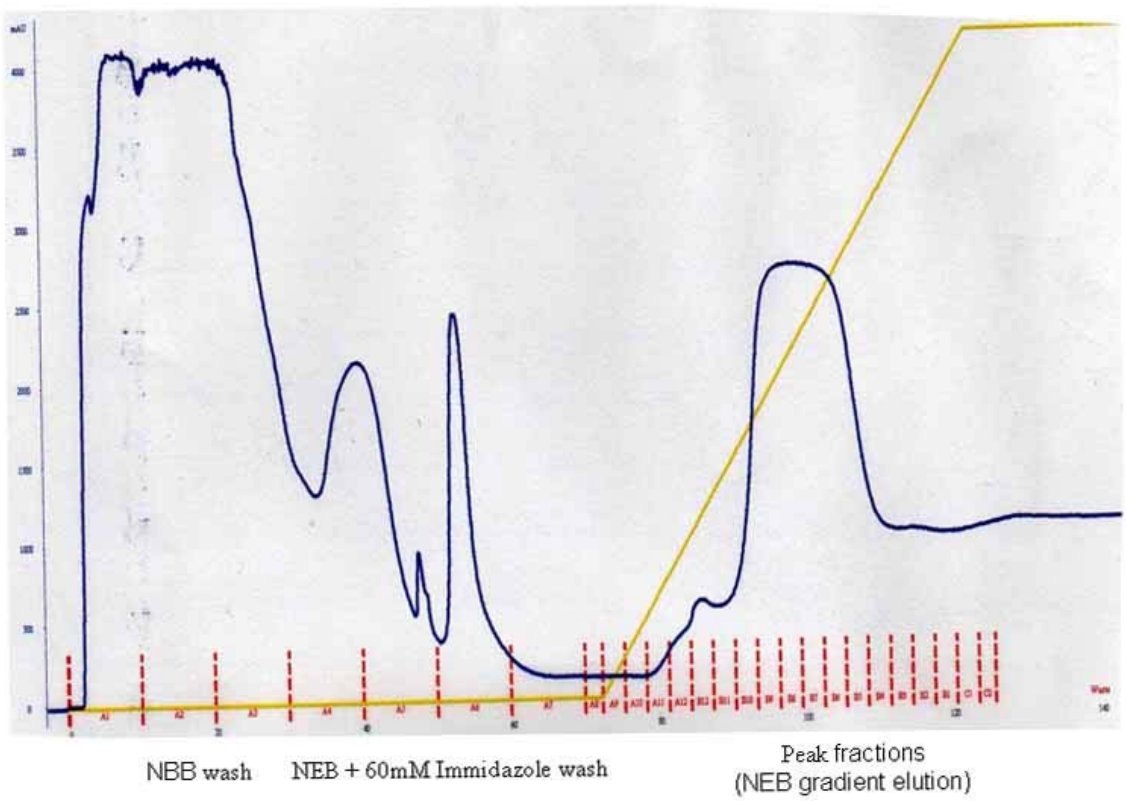

Figure 2.1: Elution profile of 30kDa from Hi-Trap chelating nickel column. The yellow line and blue lines indicates gradient concentration and absorption at A280 respectively.

Buffer Name	Buffer abbreviation	Buffer Composition	pH
Native Binding Buffer	NBB	20mM KPO_4 + 50mM NaCl + 5mM Imidazole	7.8
Native Elution Buffer	NEB	20mM KPO_4 + 50mM NaCl + 60mM/1M Imidazole	6.0
Buffer A	-------	20mM KPO_4 + 0.5mM EDTA + 7mM ß-Mercaptoethanol + 10% Glycerol + 0.1mM PMSF	6.4
Buffer B	--------	20mM Tris.HCl + 0.5mM EDTA + 7mM ß-Mercaptoethanol + 10% Glycerol + 0.1mM PMSF	7.6
Buffer C	------	20mM $NaPO_4$ + 14.4mM ß-Mercaptoethanol + 10% Glycerol + 0.1mM PMSF	6.8
Buffer D	-----	50mM Tris.HCl + 50mmM NaCl + 1mM DTT + 1mM EDTA	7.5
Buffer Q	-----	20mM bis-Tris propane + 0.5mM EDTA + 10% Glycerol	6.4
Storage Buffer	------	20mM Tris.HCl + 1mM DTT + 0.1mM EDTA + 50% Glycerol + 01mM PMSF	7.5
SDS Gel running buffer (1 liter)	------	3gm Tris.HCl + 14.4 glycine + 10 ml 10% SDS (Make up volume to 1 liter with water)	----
3.3X loading dye (10 ml)		1.5 ml 1M Tris.HCl (pH=6.8), 3ml glycerol, 3ml 10%SDS, 0.3ml ß-mercaptoethanol, 0.04 ml bromophenol blue dissolved in 2% methanol, 2.2 ml water.	
Rapid de-stain		500 ml methanol + 100 ml acetic acid + 400ml water.	

Table 2.1: Composition of Buffers

AKTA FPLC Column Variables	
Column	Hi-Trap chelating HP 5ml
Flow rate	3 ml/min
Column pressure limit	0.3 MPa
UV averaging time	5.10
Equilibration Buffer (NBB, pH=7.8) volume	10 CV
Wash Buffer (NEB + 60mM Imidazole) volume	5 CV
Flow through tube type	18mm
Equilibration/ Wash Flow through fraction size	10 ml
Protein Sample injection volume	10 ml
Elution type	Gradient elution
Elution Buffer (NEB + 60mM/1M Imidazole) volume	2 CV
Gradient	60mM Imidazole (0%) – 1M Imidazole(100%)
Elution fraction size	2 ml

Table 2.2: AKTA FPLC Hi Trap chelating column variables for the purification of 30kDa nuclease domain of RecB.

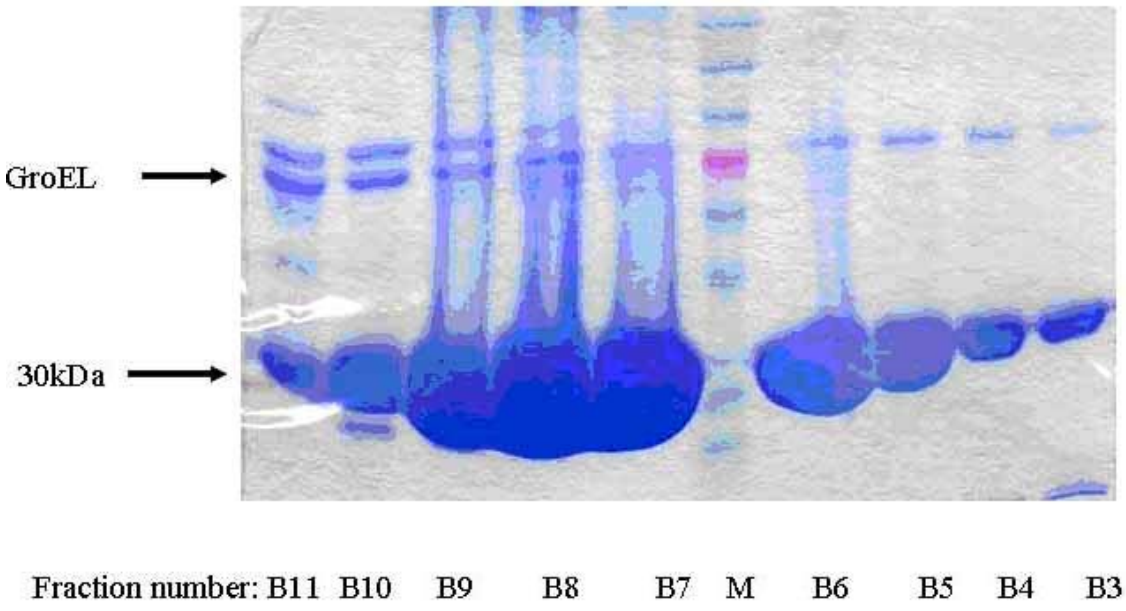

Figure 2.2: Elution peak fractions of the 30kDa fragment of RecB

2.2.2 Further purification of 30kDa by Ultra filtration:

The 30kDa copurifies with GroEL. According to the literature in Qiagen Ni-NTA his-tagged protein purification system, E. *coli* chaperonins GroEL and GroES helps in folding of the his- tagged proteins and copurifies with them. During the purification of the His-tagged 30kDa GroEL copuried and this is seen on the gel as a two bands around the 60kDa molecular weight range. Moreover, the N-terminal sequence of these bands was obtained by Zhang and Julin (unpublished work) and they corresponded to that of GroEL. Pure 30 kDa protein was obtained by ultra filtration using Centricon centrifugal filters. A Centricon YM-100 filter was used to separate GroEL from the 30kDa. GroEL is retained on the membrane and the 30kDa flows through as shown in Figure (3). A YM-10 filter is then used to concentrate the protein.

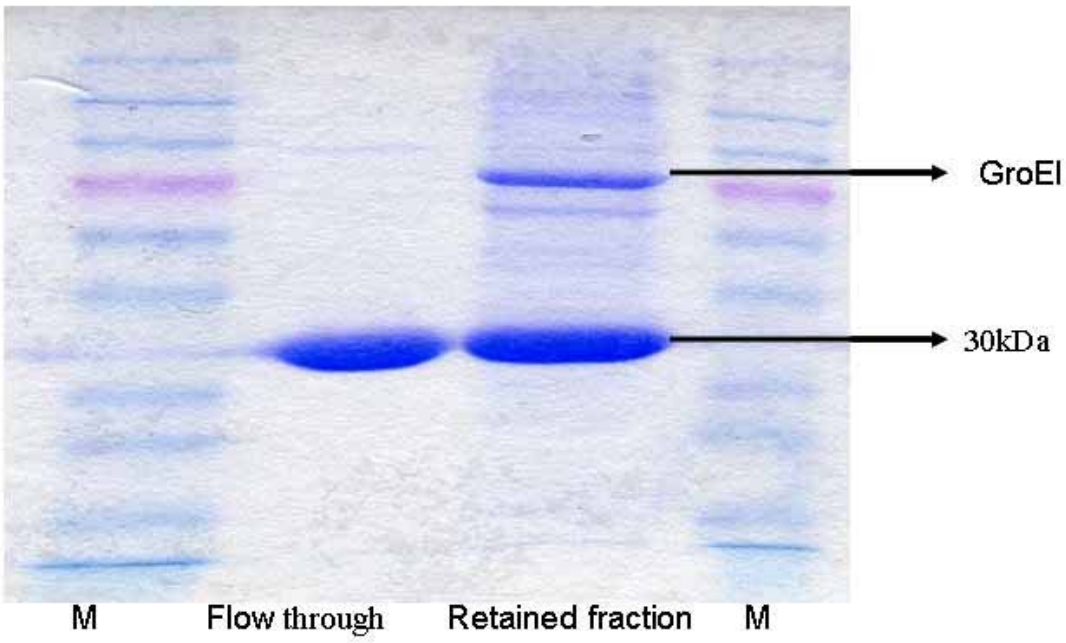

Figure 2.3: 12% SDS gel of 30kDa after ultra filtration using centricon YM-100. The 30kDa without GroEL flows through and the GroEL along with some amount of 30kDa is retained on the membrane

2.2.3 Site-directed mutagenesis:

Site-directed mutagenesis was used to construct the D1067A mutant in the 30 kDa protein. The D1080A mutant was constructed previously in our laboratory. Site-directed mutagenesis was carried out using the Quick-change site directed mutagenesis kit from Stratagene. The following primers were used,

Primer 1: 5′- CATGTTAAAAGGCTTTATCGCTCTGGTGTTCCGCC

Primer 2: 5- GGCGGAACACCAGAGCGATAAAGCCTTTTAACATG

The primers were reconstituted in 50 µl TE buffer, pH=8.0 (10 mM TrisHCl and 1mM EDTA). The primers were then gel purified before PCR. The template ds-DNA used was pET15b-30 purified from BL-21 cells by a Qiagen spin- miniprep kit. The concentration of the primers and the template DNA for the PCR was 125 ng and 20-50 ng respectively. The PCR was carried out using a PowerBlock II thermocycler (Ericomp Corp.). During the PCR, denaturation was carried out for 1min at a temperature of 95 ºC, annealing was done at 55 ºC for 1min and extension was carried out at 68 ºC for 13 min. The PCR reaction was carried out for 16 cycles. The PCR product was then digested with DpnI enzyme for 1 hour before transformation into supercompetent XL-1 blue cells. A 45 second heat pulse at 42 ºC was applied to achieve transformation of the competent cells with the PCR product. One ml SOC media was added to the cells soon after transformation and the cells were grown at 37 ºC with shaking for one hour. The transformed cells were then plated on LB-agar plates containing Ampicillin and grown overnight. A few colonies were selected from the plates and plasmid DNA

was isolated and submitted for sequencing. The mutant protein was then expressed by transforming BL-21 cells with the plasmid containing the mutation.

The solubility and expression of the 30kDa subunit was tested prior to purification. Ten milliliter cultures of the BL-21 cells expressing the protein were grown in the presence of ampicillin. The BL-21 strains containing the plasmid for D1067A was grown at 37 °C in a shaker. The cultures were grown till they reached an OD_{650} of 0.5-0.6 and induced with 1 mM IPTG for 3-4 hrs. The cells were harvested using an Eppendorf centrifuge. To determine solubility the pellets were resuspended in 20 mM HEPES buffer (pH = 7.5) and lysed using a Branson Sonicator at 30% duty cycle lasting 30 seconds for 2 cycles. To determine both the soluble and insoluble cytoplasmic fractions, the lysate obtained after sonication was centrifuged at 14,000 x g for 10 minutes in a microcentrifuge to separate the soluble and insoluble fractions. The soluble supernatant was collected. The insoluble pellet was resuspended in 500 µl of 3.3X loading dye. Both the soluble and insoluble fractions were loaded on a 12% SDS gel after adding SDS loading dye and heating for 2 min at 70 °C and stained with Coomassie blue to get an approximate measure of the soluble fraction.

2.2.4 Purification of mutant D1067A and D1080A of 30kDa protein:

Purification was carried out using Akta FPLC and the procedure is described in the Materials section above for the wild-type 30 kDa protein.

2.2.5 Fe-cleavage of the 30kDa protein:

For the experiments presented here, each enzyme was dialyzed against 40 mM Tris-HCl (pH 7.4) to equilibrate the enzyme for the cleavage reaction and to remove glycerol, which scavenges hydroxyl radicals and interferes with the Fenton chemistry. The enzyme solution was then concentrated using 4 ml Amicon Ultra-4 centrifugal concentrators. The centrifugation was carried out using a Beckman Centrifuge with a JA-10 rotor at 5000 rpm. Ferrous sulfate (0 - 1000 mM) was added to 5 - 100 μM enzyme in 40 mM Tris-HCl buffer, pH 7.4. The solution was incubated for 15 min on ice followed by the addition of ascorbate (25 mM). The solution then sat on ice or at room temperature for an additional period of 30 min to 24 h. The Fe-cleavage reactions were stopped by adding 2mM EDTA. A variety of conditions were tested, including the presence of ferrous ammonium sulfate, DTT, and hydrogen peroxide. Other conditions tested are described in detail in the results section

2.2.6 Sodium Dodecyl Sulfate-Polyacrylamide Gel Electrophoresis.

12% SDS polyacrylamide gels and Tricine-SDS polyacrylamide gels (48) were run to visualize the small products from the cleavage reactions. The Tricine – SDS gel is typically used to identify small cleavage products. The tricine SDS gel involved having a 12% separating gel and a 5% stacking gel with an anode buffer (0.2M Tris, pH= 8.9) and a cathode buffer (0.1M Tris + 0.1M Tricine +

0.1% SDS pH= 8.25). The gel apparatus had an upper and lower buffer chamber which contained the cathode and anode buffer respectively.

Electrophoresis was carried out at 35 mA at room temperature for 3 hours and destained with 50% methanol and 10% acetic acid. Molecular mass markers were used to estimate the mass of the Fe^{2+}/ascorbate-generated protein cleavage fragments that had been run on SDS-polyacrylamide gels. The protein bands were visualized by staining with 0.1% Coomassie Brilliant Blue in 50% acetic acid.

2.2.7 Isolation of Protein Fragments and N–terminal sequencing:

Peptide fragments in unstained polyacrylamide gels were electro-blotted onto Pro-Blott membranes [poly (vinylidene difluoride)] (Applied Biosystems). The electroblotting was conducted in a blotting cassette (Bio-Rad) at a constant 100 mA current for approximately 12 hours at 4°C in 0.01 M CAPS buffer, pH 11. After transfer, the protein bands were visualized by staining the membrane with 0.1% Coomassie Brilliant Blue in 50% methanol and destained with 50% methanol and 10% acetic acid. Membranes containing the transblotted protein fragments were stored at 4°C until sequencing could be performed. Automated N–terminal amino acid sequence analyses were performed by Edman degradation with an Applied Biosystems protein sequencer by Dr. Brian Martin at the National Institutes of Health.

2.3 RESULTS:

2.3.1 Optimal conditions for the Fe-cleavage reactions of the 30kDa subunit

Several sets of experiments were done under different conditions which showed that the 30kDa subunit was optimally cleaved after 30-60 min incubation at RT at pH = 7.4 in the presence of 5-100 mM ferrous sulfate, 25mM sodium ascorbate and 40mM TrisHCl. The cleavage products were visualized on a Tricine-SDS PAGE as compared to a 12% SDS PAGE.

2.3.2 Fe-cleavage of 30kda

Experiments were carried out in the presence of ferrous sulfate as literature indicated that ferrous sulfate was used in case of protein cleavage only as compared to ferrous ammonium sulfate which is used in cleaving protein – DNA complexes (49). 20µl reaction mixes were set up and incubated at 37 ºC for 180 minutes in the presence of varying concentrations of ferrous sulfate.

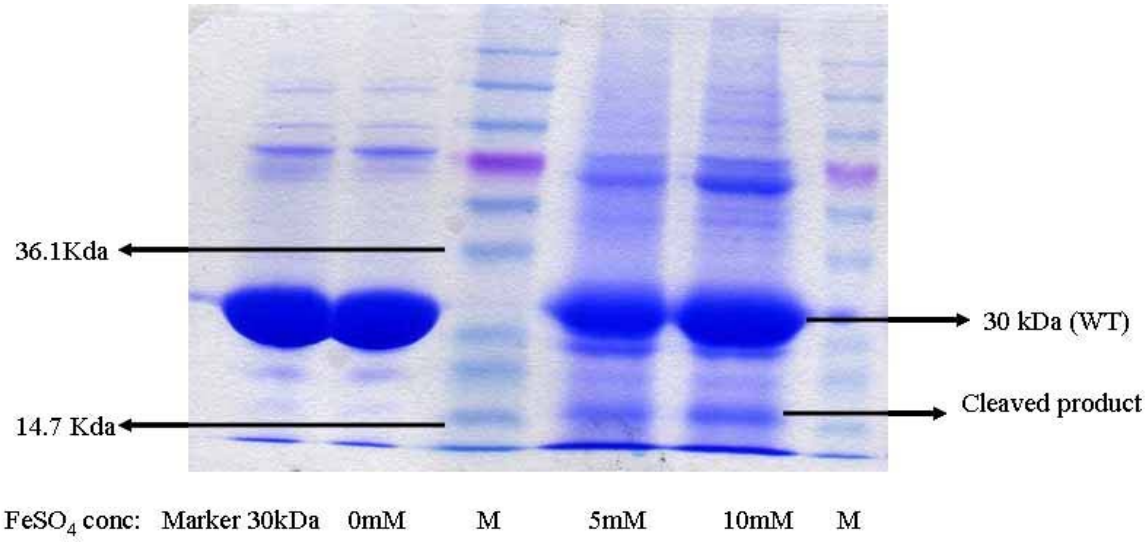

Figure 2.4: 12% SDS PAGE of 30kDa (WT) cleavage products. The reaction was incubated for 3hours with 30μM 30kDa protein, different FeSO4 concentration, 25mM Na-ascorbate and 40mM Tris buffer (pH=7.4) at RT.

The reaction mixes were analyzed in a 12% SDS gel as shown in figure (2.4). Two prominent cleavage products were visible in the 10 kDa range. However, the cleavage products were not very well resolved on a 12% SDS gel as the size of the cleaved product was very small. The Tricine-SDS gel system was used to overcome this resolution problem and further sequence the cleavage products. The cleaved products were well visualized on a Tricine-SDS PAGE gel as shown in figure (2.5) below.

2.3.3 Fe-cleavage of 30kDa: Cleavage product sequencing

In order to identify the sites where the protein was being cleaved and hence pinpoint the metal-binding site a Tricine-SDS gel was run. This gel is typically used to identify small cleavage products. The cleavage products were visualized well on a Tricine SDS gel and a sequence was obtained by Edman sequencing. The sequencing data showed that the cleavage was occurring near Asp1067 which is one of the crucial residues in the nuclease active site of the nuclease domain of RecB. It suggests that Asp1067 is involved in metal binding. The other band in the gel that was sequenced had a sequence of G S S H H H which corresponded to the His-tag of the 30kDa nuclease fragment of RecB. The sequences obtained were G S S H H H (Band 2, Fig 2.5)
I D L V F R H E G R (band 3, Fig 2.5) and S P G T F L H S L (band 1, Fig 2.5). The sequence of band 1 agrees with the amino-terminal sequence of the His-tagged 30kDa, lacking the initial methionine residue. We found previously (Zhang and Julin, unpublished data) that the mass of the purified 30kDa protein

was consistent with loss of the amino terminal Met residue. The amino-terminal sequence for the middle band agrees with residues # 1066 – 1075 of the full-length RecB protein (residues # 160 – 169 of 30kDa). The second residue (D) of this peptide is Asp1067 of RecB, previously shown to be important for the nuclease activity of RecB (33). The result suggests that the iron is bound in the vicinity of amino acid #1066 of the 30kDa nuclease domain. The sequence obtained for the topmost band (band 1) corresponds to residues # 950 – 958 of RecB protein (residues # 44 – 52 of 30kDa nuclease domain).

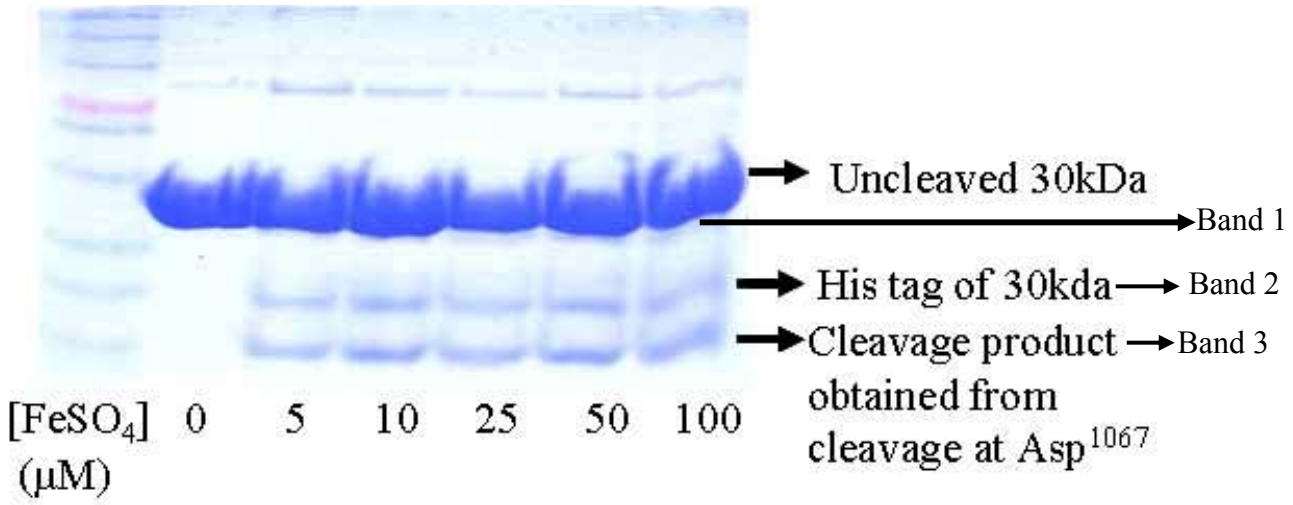

Figure 2.5: Tricince-SDS gel showing the cleavage products of the 30kDa protein at different concentrations of $FeSO_4$.

2.3.4 Fe-cleavage reaction in the presence of different metals

To study the effect of different metals on the cleavage reactions, the Fe-cleavage reaction was done in the presence of varying concentrations of magnesium chloride and calcium chloride. 30kDa protein (50 μM) was incubated with ferrous sulfate/sodium ascorbate in 40 mM Tris buffer (pH=7.4) at RT. The reaction was quenched by the addition of 2mM EDTA and the cleavage products were analyzed on a Tricine-SDS gel.

2.3.4.1 Fe-cleavage reaction in the presence of $MgCl_2$

The band corresponding to the cleavage at Asp1067 is faint at high concentrations of Mg^{2+} as shown in figure (2.6). The cleavage products are formed at a slower rate in presence of $MgCl_2$. This also indicates that magnesium does not bind very tightly to the binding site.

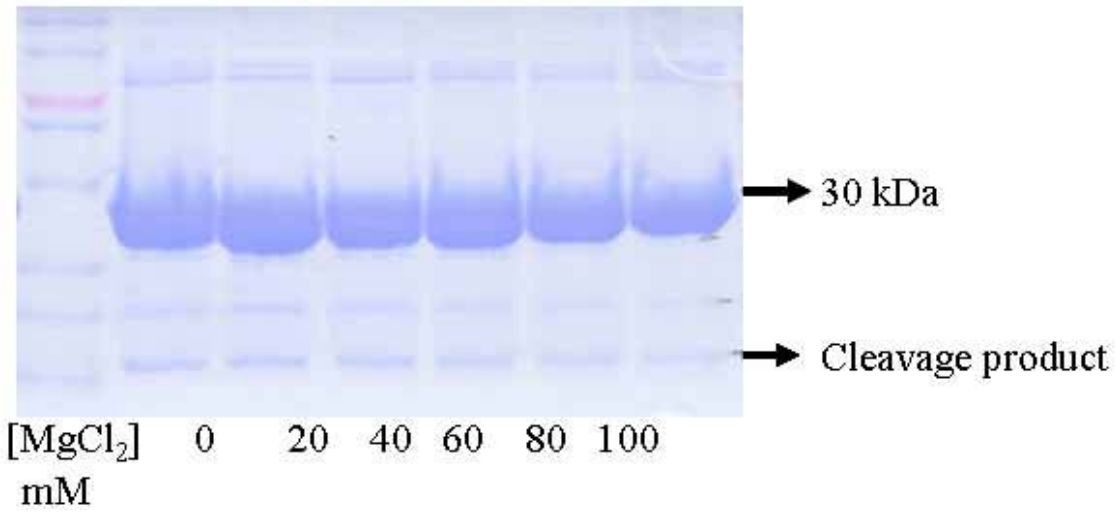

Figure 2.6: Cleavage of 50µM 30 kDa in presence and absence of $MgCl_2$, 5µM $FeSO_4$ and 25mM Na-ascorbate

2.3.4.2 Fe-cleavage reaction in the presence of $CaCl_2$:

Calcium is an inhibitor of the nuclease activity of the 30kDa nuclease domain of RecBCD (39).Cleavage of 30kDa is completely inhibited in the presence of $CaCl_2$ as shown in figure (2.7). This suggests that Ca^{2+} binds to the metal binding site located in the vicinity of Asp1067 and inhibits Fe^{2+} from binding. This set of experiments also suggests that calcium binds to the nuclease active site much more strongly than magnesium.

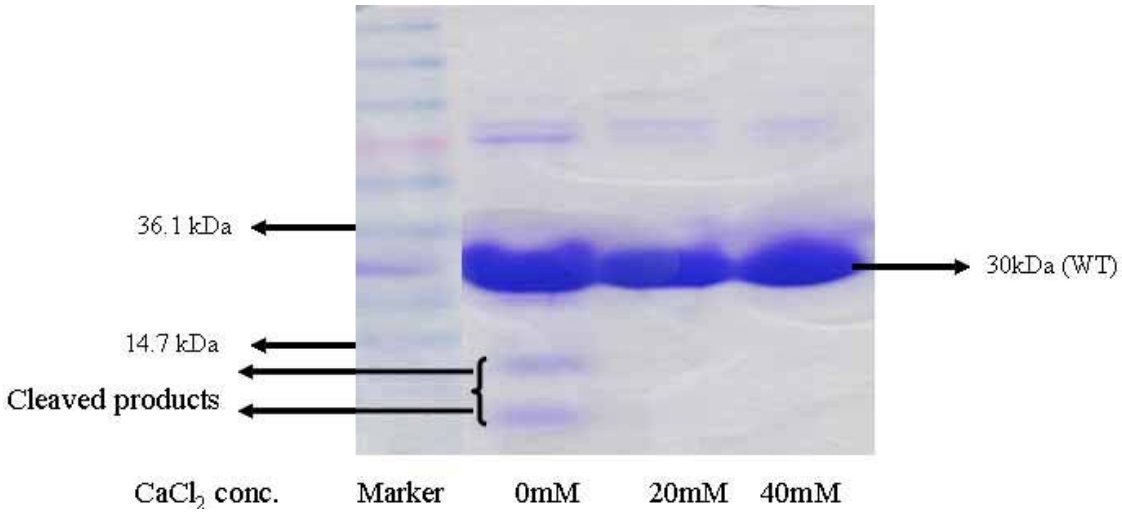

Figure 2.7: Cleavage of 50µM 30 kDa in presence and absence of $CaCl_2$, 5µM $FeSO_4$ and 25mM Na-ascorbate at RT.

2.3.5 Fe-cleavage of 30kDa mutant (D1067A mutant of 30kDa):

The following study was done to assess the effect of the Fe-induced cleavage on the mutant protein. Wild-type 30kDa and the D1067A mutant protein (50 μM) were incubated with 5 μM $FeSO_4$ and 25 mM sodium ascorbate for the indicated time at RT. The reaction was quenched by the addition of 2 mM EDTA and the cleavage products were analyzed on a Tricine-SDS gel (Figure 2.8). The formation of cleavage products in the mutant was absent indicating that the mutation has altered the metal binding site, thus preventing the metals from binding.

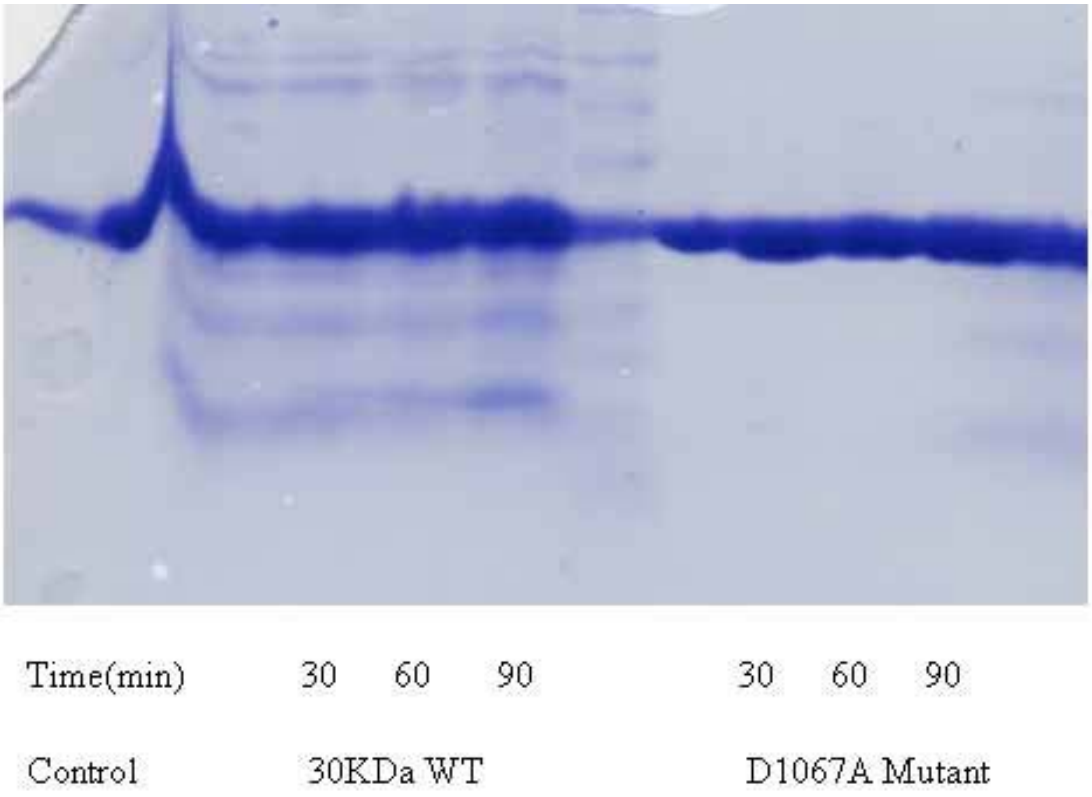

Figure 2.8: Comparison of Fe-cleavage reactions of the 30kDa WT and D1067A mutant of 30kDa.

2.3.6 Fe-cleavage of 30kDa mutant (D1080A mutant of 30kDa):

Fe-cleavage reactions were carried out with a mutant of the 30kDa nuclease domain where the aspartate residue at position 1080 was mutated to an alanine. This aspartate residue was earlier shown to be required for the nuclease activity of RecBCD (50). The figure (2.9) below shows that the cleavage reaction is not inhibited in the case of the D1080A mutant indicating that aspartate 1080 is not involved in magnesium metal binding. The reaction conditions are described in the materials section.

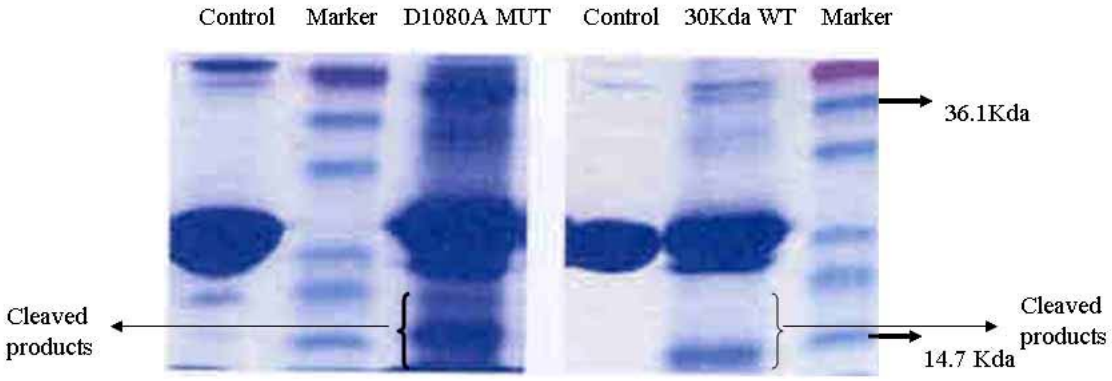

Figure 2.9: Comparison of Fe-cleavage reactions of the 30kDa WT and D1080A mutant of 30kDa.

2.4 DISCUSSION:

Alignment of C-terminal sequence of *E. coli* RecB protein with homologous proteins from other bacteria identified conserved aspartates at position 1067 and 1080 and a lysine at position 1082. Mutation of the amino acid residues Asp^{1080}, Asp^{1067} and Lys^{1082} abolished nuclease activity on both single and double stranded DNA (51). These residues compose a motif that is similar to one shown to form the active site of several restriction endonucleases (Figure 2.10) (33). Mg^{2+} ion has been shown to play a role in the activity of nucleases containing acidic residues in their active site.

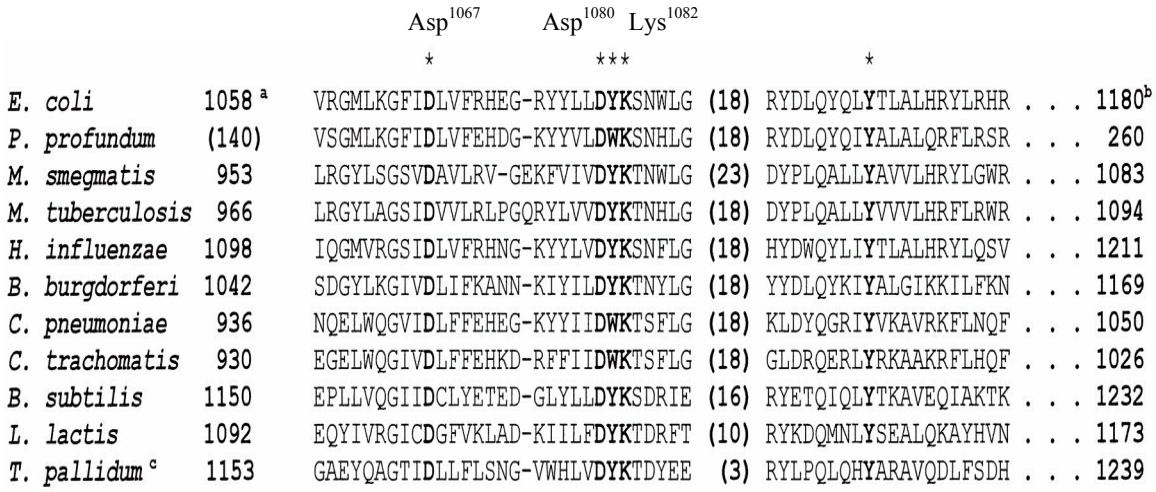

Figure 2.10**:** Alignment of C-terminal sequence from the *E. coli* RecB protein with homologous proteins from other bacteria.

The Fe-cleavage technique was used to map the metal binding sites in several DNA binding enzymes like restriction endonucleases (42), DNA primase (52), and RNA polymerase (49). The identification of metal binding site of an enzyme using this technique helps in identifying the precise metal binding site in the structure of the enzyme. The work presented in this chapter was done before the crystal structure of RecBCD was published (38). The Fe-cleavage experiments showed that magnesium bound to the aspartate at position 1067. Iron and magnesium both have a divalent metal ion chemistry and it is possible that their mode of binding to the protein is very similar. Hence, the Fe-cleavage tells us where the iron binds and we assume this is the place where magnesium binds too. Cleavage reactions with mutant aspartate residue at 1067 inhibit cleavage product formation as compared to mutation at aspartate 1080. A mutation at aspartate 1080 inhibits nuclease activity but does not have any effect on magnesium binding. This suggests that there is a unique magnesium binding site in the nuclease domain of RecB.

Type II restriction endonucleases are enzymes which protect bacteria against foreign DNA by cleaving it. These enzymes have a nuclease active site which is responsible for cleaving the DNA. The active site of 30kDa nuclease domain of RecB has many similarities with these restriction endonucleases. Sequence alignment show that both the 30kDa and the nuclease domain have the PD . . . D/ExK motif in their active site. The active site in the 30kDa is made up of Asp 1062, Asp 1080 and Lysine 1082.

Calcium metal ion is bound in the RecBCD crystal structure. The crystal structure of RecBCD was obtained in the presence of calcium acetate and not magnesium. This was because calcium binds to the nuclease active site of RecBCD more tightly than magnesium. Our results with the Fe-cleavage showed that the cleavage reaction was inhibited in the presence of Calcium and not to a large extent in presence of magnesium. Moreover, the calcium ion in the crystal structure is seen bound to the side chains of His956, Asp1067, and Asp1080, in the nuclease domain of RecB. We do not detect a cleavage product near Asp1080 of the 30kDa and mutation of Asp1080 does not abolish the cleavage that occurs near Asp1067. This is significant since Asp1080 is a calcium ion ligand in the RecBCD crystal and it is important for RecBCD nuclease activity. This result suggests that the two acidic residues contribute differently to the overall metal ion binding under the conditions of the iron-cleavage reactions. Examination of the active site structure and the location of the cleavage sites suggest a possible explanation. The amino acid residues from which C_{α}-H abstraction would initiate peptide bond cleavage are on the opposite side of Asp1067 and Asp1080. Instead, they are closer to Glu1020, the residue that is structurally analogous to the acidic residue that is in metal ion binding site II in some enzymes (Fig 2.11). This suggests that the iron responsible for the cleavages could be bound in a site that involves Asp1067 and, perhaps, Glu1020. Further, this would indicate that RecBCD can bind metal ions in several ways, in addition to that observed in the crystal structure. The technique of Fe-cleavage was mainly used to study metal binding sites to which the metal was known to bind tightly. The success of this

technique in our system illustrates that the technique of Fe-cleavage to metal binding sites can be used for the study of metal binding sites with different affinities to their respective metals.

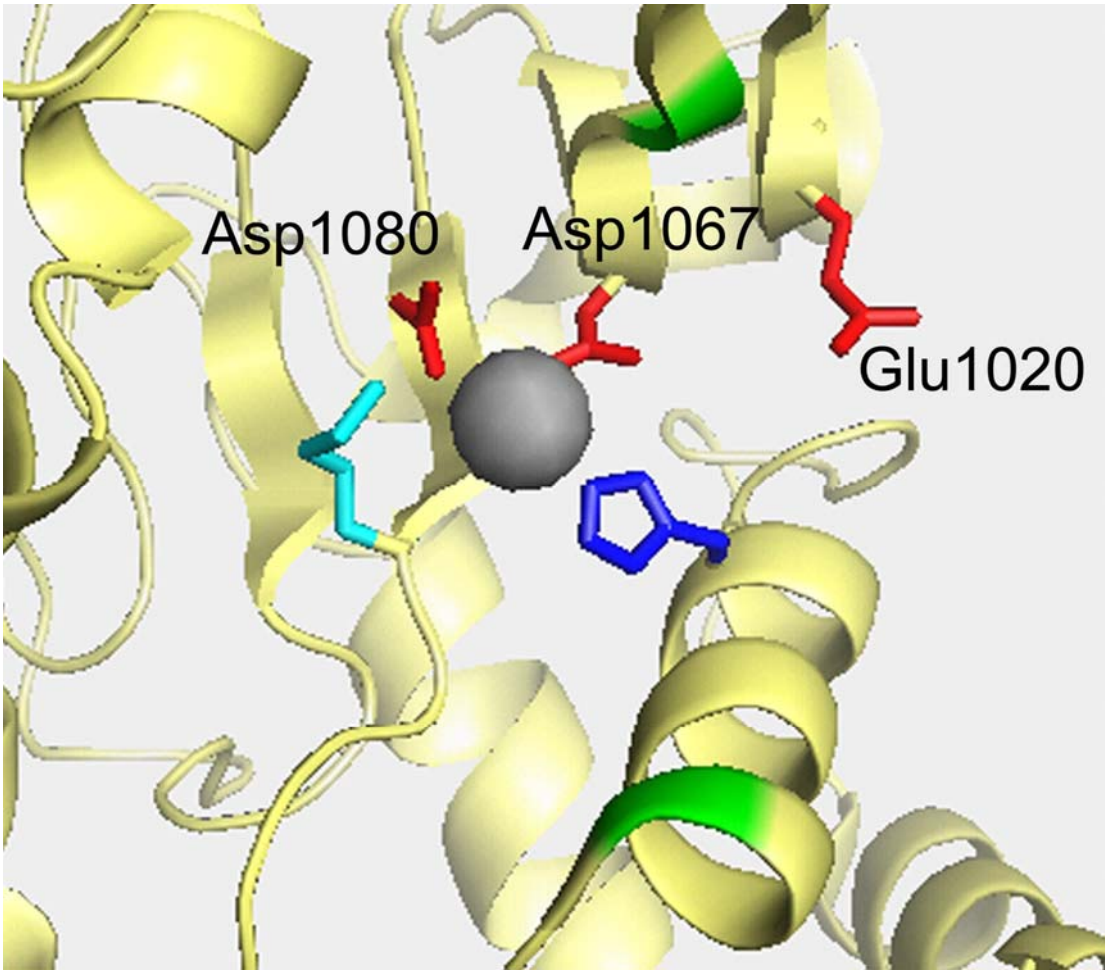

Figure 2.11: Model of the RecBCD Nucleus and Metal binding site. The amino acids labeled in red are aspartate 1080 and aspartate 1067. Histidine 956 is indicated by blue and lysine1082 is indicated in cyan. The gray sphere is calcium. The green color indicates the peptide bonds that are cleaved. (Dr.DA Julin)

3 Chapter 3: The Role of Magnesium in the Subunit Interactions of RecBCD and Iron Cleavage of 100kDa Helicase Domain of RecBCD

3.1 Introduction

The RecB protein has a 30kDa C-terminal nuclease domain and a 100kDa N-terminal helicase domain. RecBCD is a dsDNA dependent ATPase and an ATP dependent helicase and exonuclease. Dixon et al. showed that in presence of DNA containing chi sequences and limiting concentrations of magnesium, RecBCD is incapable of unwinding intact DNA molecules. However, this inactivation of the unwinding activity is reversible upon the addition of 10mM Mg^{2+}. Also, upon the subsequent increase of Mg^{2+} concentration the degradative nuclease activity is fully reversible. Moreover, they also showed that chi inactivated RecBCD does not unwind DNA at low concentrations of Mg^{2+}.

Taylor et al (40) showed that the RecBCD enzyme gets inactivated upon encountering chi containing DNA. The inactivation was reversible upon addition of magnesium in excess of ATP. Ultracentrifugation analysis of the RecBCD after it encountered chi showed that the enzyme disassociated into three subunits RecB, RecC and RecD. The RecB was bound to DNA and the RecD formed aggregates when they sedimented.

Preliminary work done in our research group by Dr. Olga Carlson indicated that magnesium in presence of DNA enhanced the binding of 100kDa and RecC. The study by Dixon et al, Taylor et al. and preliminary work done in our laboratory corroborated that the presence of magnesium was essential for the

activity of the RecBCD enzyme. The figures (3.1 & 3.2) shown in Dr.Carlson's result show that the RecC and the 100kDa remained as tightly bound complex in presence of ss-DNA and 20mM magnesium chloride. This effect is not seen on the nickel column.

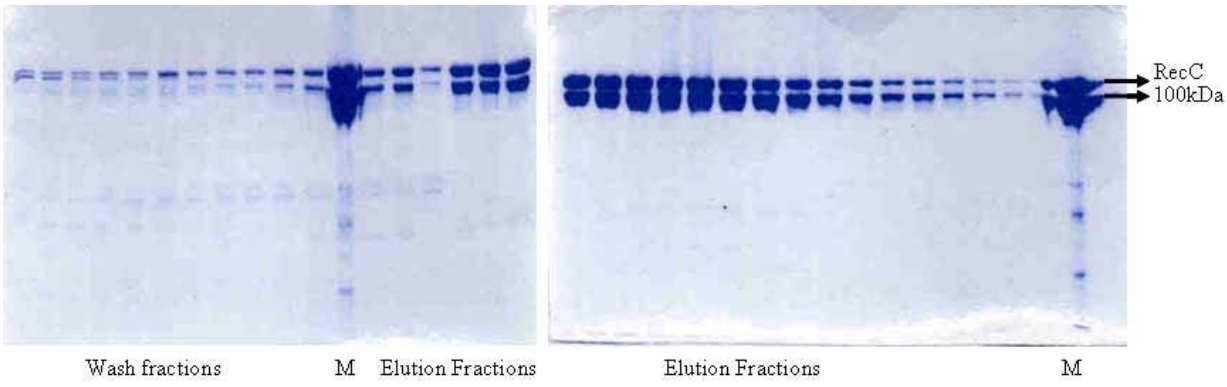

Figure 3.1: Nickel column fractions of 100kDa-RecC complex. The column was eluted in the absence of magnesium.

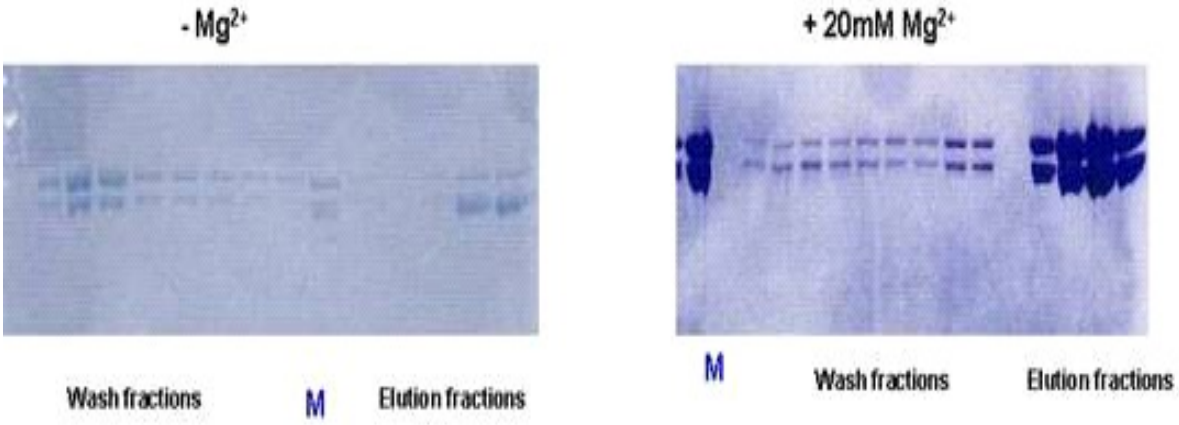

Figure 3.2: ssDNA-agarose column fractions of 100kDa-RecC complex. The column was eluted in the absence and presence of 20mM of magnesium.

In an effort to understand the interactions between the RecB and RecC subunits of *E. coli* we studied how magnesium played a role in this interaction. The crystal structure of RecBCD was solved recently and it showed that the RecC contains three large channels that run through the protein (38). RecB has been identified as a member of the SF1 super family of helicases, which are comprised of other helicases as PcrA and Rep (53). The crystal structure of RecBCD has shown that the structure of the amino terminal of the RecB has regions similar to the canonical 1A, 1B, 2A and 2B of other SF1 helicases. The 2B domain is the only domain that does not contain any of the conserved amino acids that comprise the seven so-called "helicase motifs" that define the SF1 helicase superfamily.

The largest of these channels accommodates the 2B domain of RecB and provides a major interface between the proteins. The other two channels are pathways along which the single-stranded tails of the DNA run to, or from, the two helicase subunits. Moreover the domain 2B of RecB is also located in the 100kDa N-terminal of the RecB protein. The 100kDa fragment is a helicase domain and magnesium is required for the helicase to function. Fenton chemistry techniques were used to probe whether magnesium had a binding site in the helicase domain. We adopted a two-pronged strategy and multiple techniques to get an insight into the effect of magnesium in the interactions between RecB and RecC. Direct binding changes between RecB and RecC in presence and absence of magnesium were measured using ss-DNA-agarose column chromatography, Biacore, Nickel spin columns and gel filtration.

3.2 Materials and Methods

3.2.1 Expression of 100kDa helicase domain

The 100kDa was His-tagged at the N–terminus. The solubility and expression of the 100kDa subunit was tested prior to its purification. The M-15 strains contained the pRep4/OC-2 plasmid expressing the 100kDa and were grown in LB media at 30 °C with vigorous shaking at shaker speeds of 250-300 rpm. Each batch of purification was done using a culture of volume 2 - 10 liters. An overnight 50ml seed culture was grown to saturation. This saturated culture was used to start the larger cultures the next day. The dilution was 1:200. The cells were grown till the OD_{650} was 0.5-0.6. Induction was carried out with 1mM IPTG for 4-5 hours. The cells were harvested in a Beckman centrifuge using a JA-10 rotor at 10,000 rpm for 10 minutes. The pelleted cells were stored at –80 °C . The cells were lysed the next day after re-suspending the pellet in 5-10ml of NBB. Protease inhibitor cocktail (Sigma) was added to the re-suspended cells before lysis. Cell lysis was done using a Branson 3000 Sonicator at a duty cycle of 30% for 30 seconds for an average of 10-15 cycles. Care was taken so that frothing did not take place during cell lysis using sonication. The lysate was cleared by centrifuging the crude cell lysate at 20000 rpm using a JA 20 rotor for 90 minutes at 4 °C in a Beckman centrifuge. The lysate was then decanted into a polypropylene tube and filtered using a 0.22 micron syringe filter. It is important to filter the crude lysate before loading on the FPLC columns to avoid clogging of the filters.

3.2.2 Purification of 100kDa helicase domain using FPLC

Purification of the 100kDa was done using an Amersham Pharmacia FPLC system and columns. The composition of the buffers and purification parameters for the different columns are listed in Table (3.1). The crude lysate was loaded on a 5ml Hi-Trap chelating nickel column using a 10ml or 150ml Superloop. Depending on culture volume up to three Hi-Trap nickel columns were used. This was done by connecting the columns in a series using adaptors. The column was then washed with NBB (pH=7.8) to enable binding of the His-tagged 100kDa to the column. Unbound protein was washed out with NEB + 60mM imidazole (pH=6.0). The protein was gradient eluted using NEB (pH=6.0) with a gradient of 60mM-1M imidazole. The eluted fractions were collected in several tubes using a fraction collector (Figure 3.3 & 3.4). The peak fractions containing the protein were pooled and dialysed in Buffer D (pH=7.5) for loading on a 5ml Hi-Trap heparin column. Again depending on the volume of the pooled fractions and protein concentration 1-2 Hi-Trap heparin columns were used. After loading the protein on the column it was washed with Buffer D (pH=7.5). Gradient elution was done using BufferD (pH=7.5) with a gradient of 0-1M NaCl. The peak fractions were collected using a fraction collector (Figure 3.5 & 3.6). Twenty microlitres of each fraction was loaded on a 12% SDS-PAGE to check for purity. The fractions containing pure protein were pooled and dialysed in the storage buffer (pH=7.4) (Table 3.1) for the 100kDa. The purified 100kDa typically had concentrations of 4-10μM. The protein was stored at -80ºC.

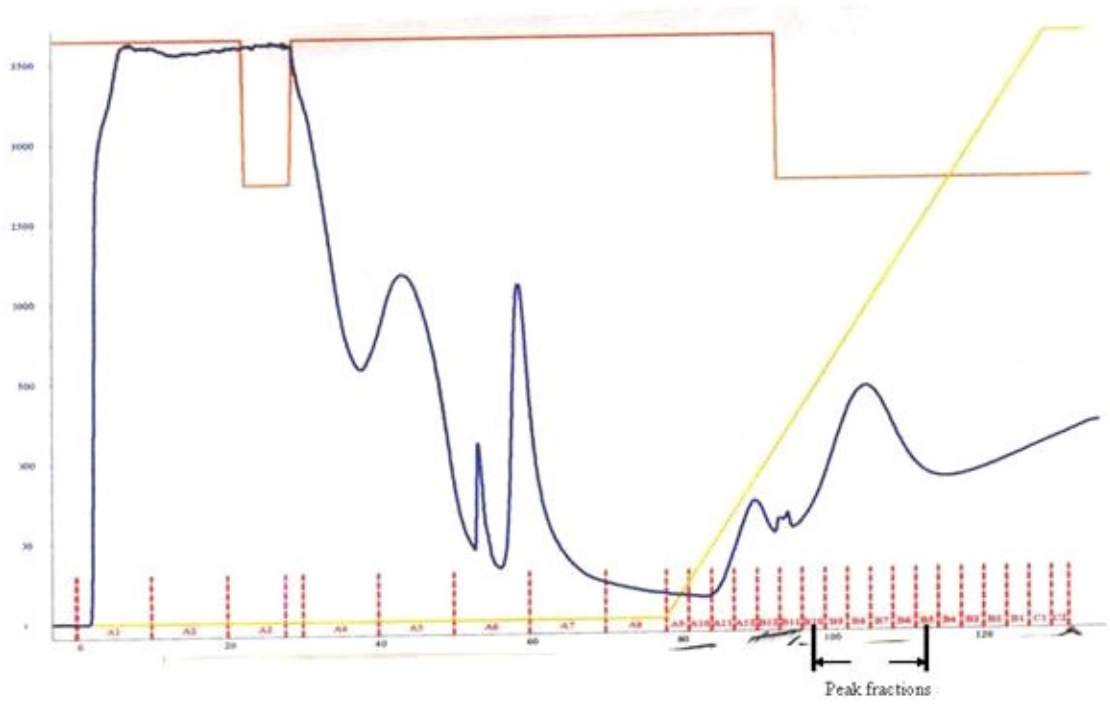

Figure 3.3: Elution profile of 100kDa from Hi-Trap chelating nickel column. The red line, yellow line and blue line indicate flow-rate, gradient concentration and absorption at 280 nm respectively.

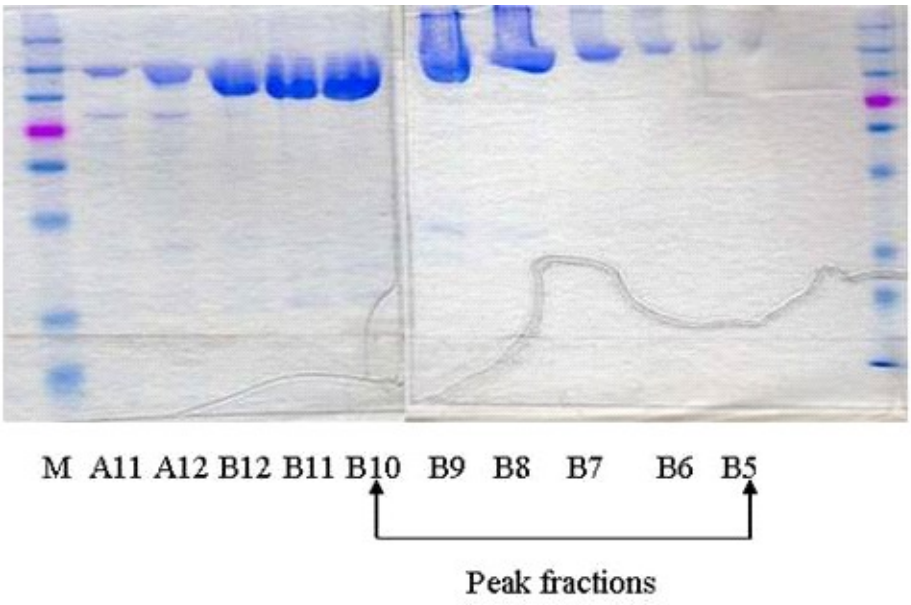

Figure 3.4: 12% SDS PAGE of 100kDa fractions from Hi-Trap Nickel column.

Buffer Name	Buffer abbreviation	Buffer Composition	pH
Native Binding Buffer	NBB	20mM KPO_4 + 50mM NaCl + 5mM Imidazole	7.8
Native Elution Buffer	NEB	20mM KPO_4 + 50mM NaCl + 60mM/1M Imidazole	6.0
Buffer A	-------	20mM KPO_4 + 0.5mM EDTA + 7mM ß-Mercaptoethanol + 10% Glycerol + 0.1mM PMSF	6.4
Buffer B	--------	20mM Tris.HCl + 0.5mM EDTA + 7mM ß-Mercaptoethanol + 10% Glycerol + 0.1mM PMSF	7.6
Buffer C	------	20mM $NaPO_4$ + 14.4mM ß-Mercaptoethanol + 10% Glycerol + 0.1mM PMSF	6.8
Buffer D	-----	50mM Tris.HCl + 50mmM NaCl + 1mM DTT + 1mM EDTA	7.5
Buffer Q	-----	20mM bis-Tris propane + 0.5mM EDTA + 10% Glycerol	6.4
Storage Buffer	------	20mM Tris.HCl + 1mM DTT + 0.1mM EDTA + 50% Glycerol + 01mM PMSF	7.5
SDS Gel running buffer (1 liter)	------	3gm Tris.HCl + 14.4 glycine + 10 ml 10% SDS (Make up volume to 1 liter with water)	----
3.3X loading dye (10 ml)		1.5 ml 1M Tris.HCl (pH=6.8), 3ml glycerol, 3ml 10%SDS, 0.3ml ß-mercaptoetanol, 0.04 ml bromophenol blue dissolved in 2% methanol, 2.2 ml water.	
Rapid de-stain		500 ml methanol + 100 ml acetic acid + 400ml water.	

Table 3.1: Composition of Buffers

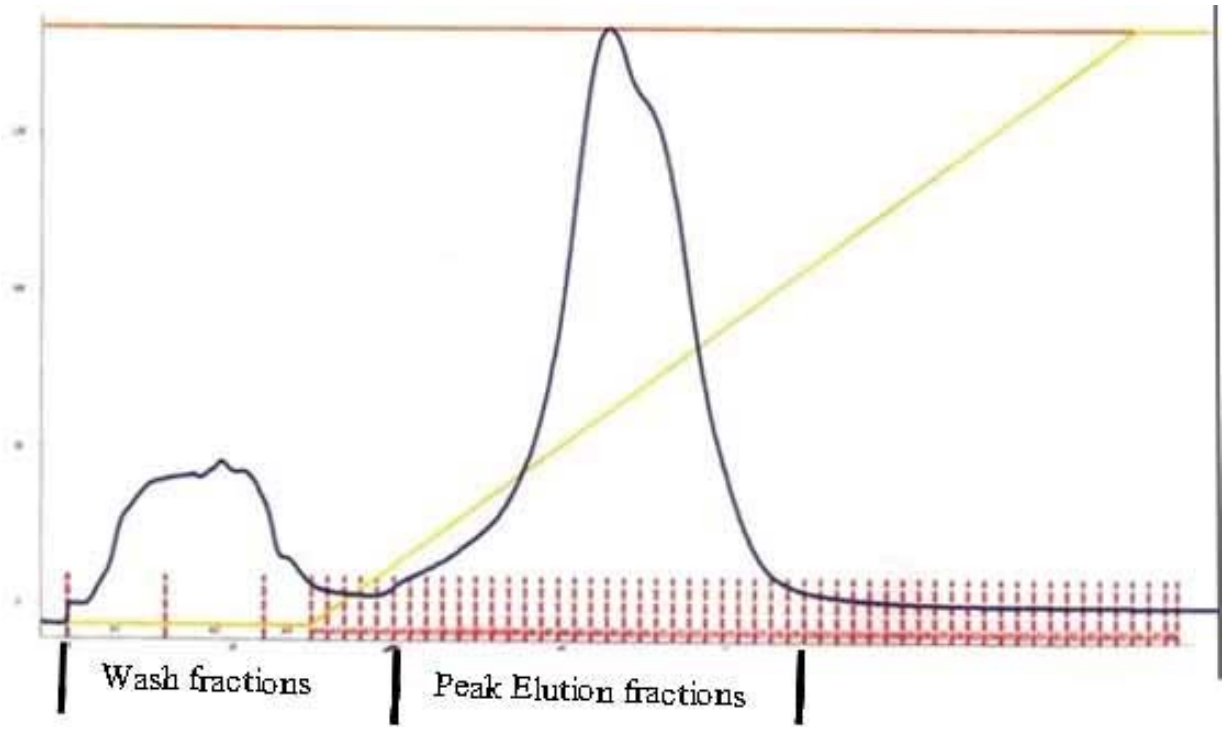

Figure 3.5: Elution profile of 100kDa from Hi-Trap heparin column. The red line, yellow line and blue line indicate flow-rate, gradient concentration and absorption at 280 nm respectively.

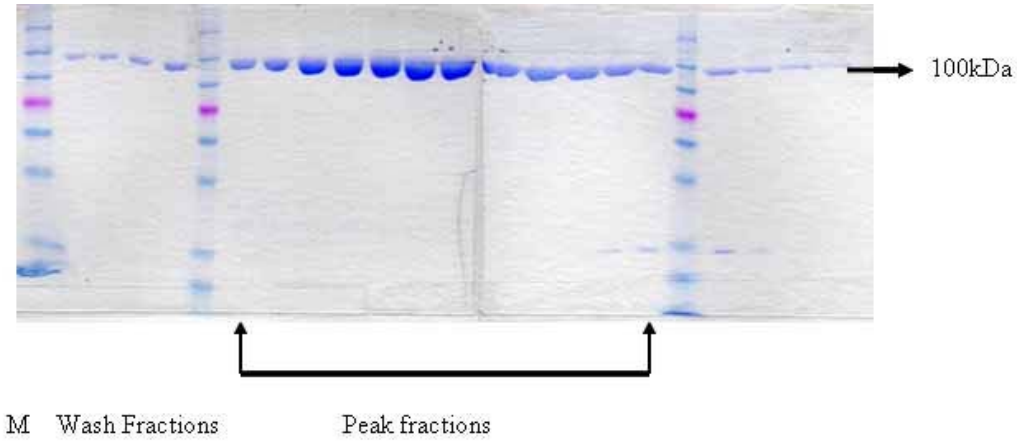

Figure 3.6: 12% SDS PAGE of 100kDa fractions from Hi-Trap heparin column. M stands for the pre-stained invitrogen marker.

3.2.3 Expression of RecC subunit

The RecC protein was expressed from V186 cells containing the plasmid pNM52/pPB500. V186 is an *E.coli* strain which is deficient in RecBCD. The pPB500 encode the RecC protein and the pNM52 encode the *lac* repressor. The solubility and expression of the RecC subunit was tested in smaller culture volumes of 10ml prior to its purification. The V186 strain expressing the RecC subunit was grown in 2xYT (5gm yeast, 5 gm tryptone and 2.5gm NaCl dissolved in 250 ml water) media containing ampicillin (50mg/ml), tetracycline (15mg/ml) and thymidine (50mg/ml) at 37 °C with vigorous shaking at shaker speeds of 250-300 rpm. Since the V186 cells were mutants deficient in recombinational repair, it was hard to get good expression of the RecC protein. Each batch of purification was done using a culture volume of 2 - 10 liters. An overnight 50ml seed culture was grown to saturation. This saturated culture was used to start the larger cultures the next day. The dilution was 1:200. The cells were grown till the OD_{650} was 0.5-0.8. Higher OD yielded higher levels of expressed RecC. The cells were then induced with 1mM IPTG for 3 hours. The cells were harvested in a Beckman centrifuge using a JA-10 rotor at 10000 rpm for 10 minutes. The pelleted cells were stored at –80 °C . The cells were lysed the next day after re-suspending them in Buffer A. Protease inhibitor cocktail (Sigma) was added to the re-suspended cells before lysis. Cell lysis was done using a Branson 300 Sonicator at a duty cycle of 30% for 30 seconds for an average of 10-15 cycles. Care was taken to so that frothing did not take place during cell lysis using sonication. The lysate was cleared by centrifuging the crude cell lysate at 20000

rpm using a JA 20 rotor for 90 minutes at 4 °C in a Beckman centrifuge. Precipitation of the protein from the lysate was carried out by slow addition of crushed 30% ammonium sulfate for a period of 1 hour at 4ºC. The protein from the lysate was pelleted by centrifuging at 15000 rpm for 90 minutes using a JA-10 rotor in a Beckmann centrifuge. After the pellet was obtained it was redissolved in 3ml of Buffer A and dialysed against Buffer A. The protein solution was filtered using a 0.22 micron syringe filter before loading on the FPLC columns.

3.2.4 Purification of RecC subunit using FPLC:

Purification of the RecC subunit was done using an Amersham Pharmacia FPLC system and columns. The composition of the buffers is listed in Table (3.1). The protein solution was loaded on a 5ml Q_FF6 (Q-Sepharose) anion-exchange column. Depending on the culture volume multiple columns were used. The column was washed with Buffer A and the protein was eluted using a gradient of 0-450mM NH_4Cl. The peak fractions were collected and 20µl of each fraction was run on a 12% SDS gel (Figure 3.7 and 3.8). The peak fractions containing the protein were pooled and dialyzed against Buffer B for loading on a heparin column. The protein solution was loaded on a 5ml Hi-Trap heparin column using a 150ml Superloop.

The column was washed with Buffer B and the protein was eluted by applying a gradient of 0-1M NaCl. The peak fractions were collected and 20µl of each fraction was run on a 12% SDS gel (Figure 3.9 and 3.10).. Peak fractions containing RecC were pooled and dialysed in Buffer C for loading on a Hydroxyapatite column. The protein solution was loaded on a 10 ml CHT5

hydroxyapatite column from Bio-Rad. The column was attached to the Pharmacia FPLC system using adaptors provided by Bio Rad. The column was washed with Buffer C and the protein was eluted using a gradient of 20-250mM $NaPO_4$. The peak fractions were collected and 20µl of each fraction was run on a 12% SDS gel. The peak fractions containing the protein were pooled together and dialysed against Buffer Q for further purification using a MonoQ column. The protein solution was loaded on a 5ml MonoQ HR 5/5 column using a 10ml Superloop. The column was washed with Buffer Q and the protein was eluted using a gradient of 0-500mM KCl. The peak fractions were collected and 20µl of each fraction was run on a 12% SDS gel (Figure 3.11).. The peak fractions containing the protein were pooled together and dialysed in the storage buffer. The purified RecC was stored at -80ºC.

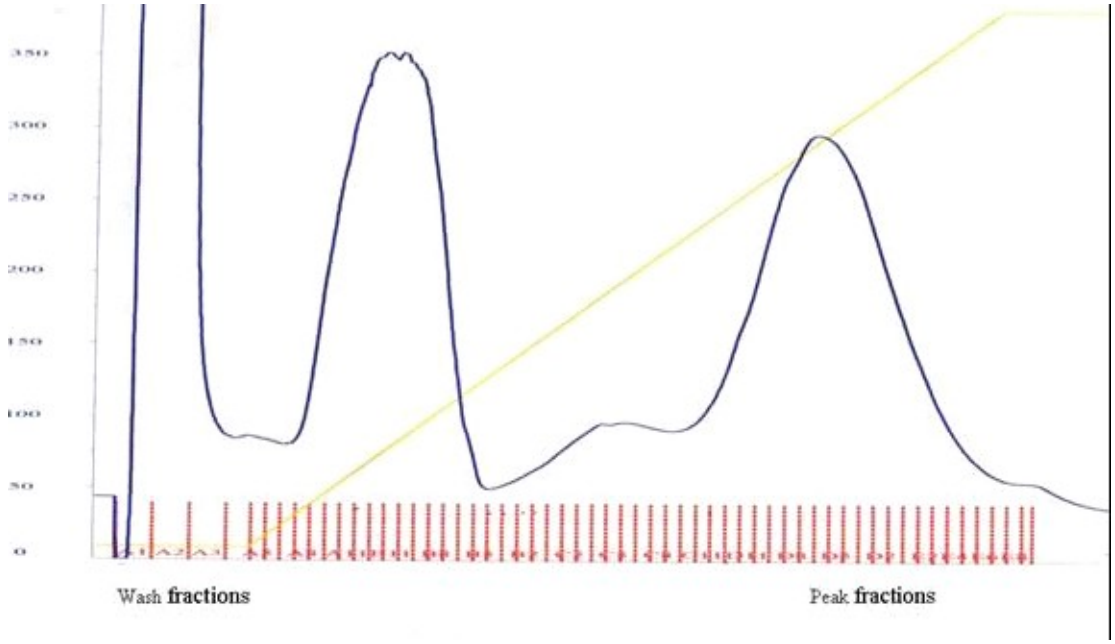

Figure 3.7: Elution profile of RecC from Hi-Trap QFF column. The red line, yellow line and blue line indicate flow-rate, gradient concentration and absorption at 280 nm respectively.

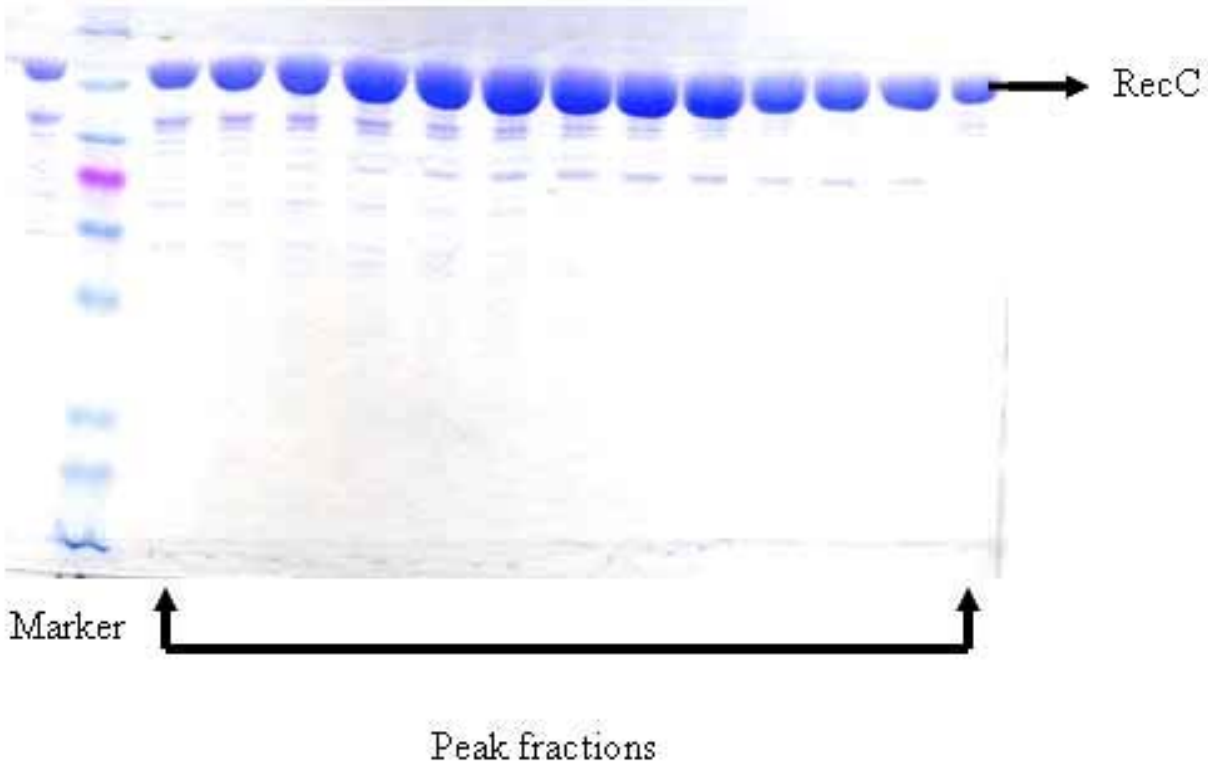

Figure 3.8: 12% SDS PAGE of RecC peak fractions from Hi_Trap QFF column.

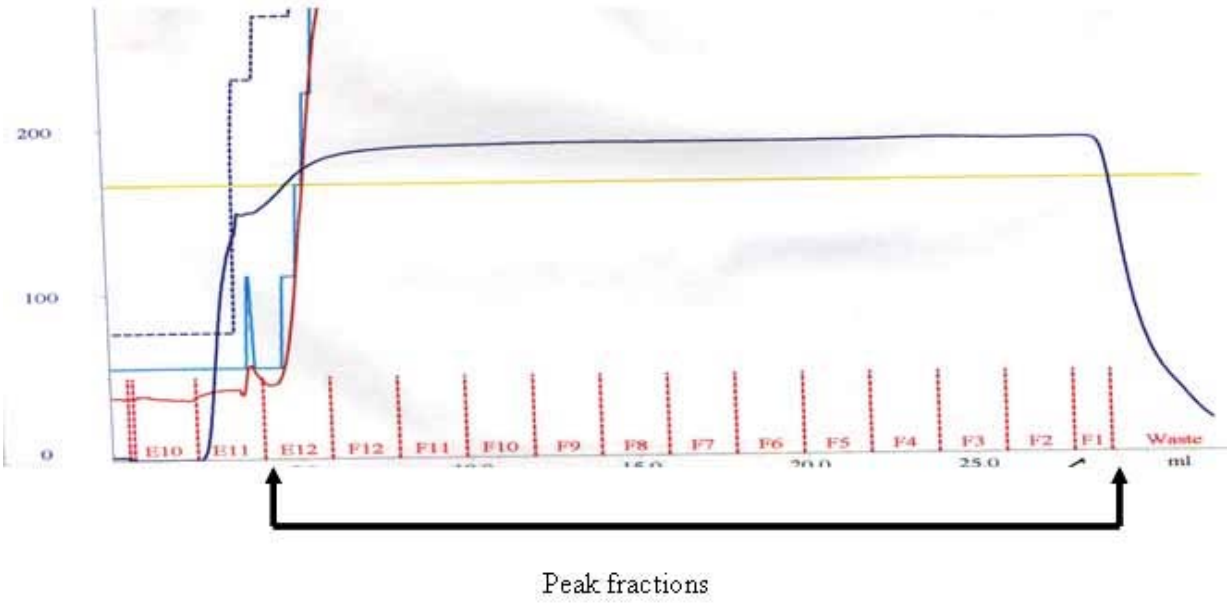

Figure 3.9: Elution profile of RecC from Hi-Trap heparin column. The red line, yellow line and blue line indicate flow-rate, gradient concentration and absorption at 280 nm respectively.

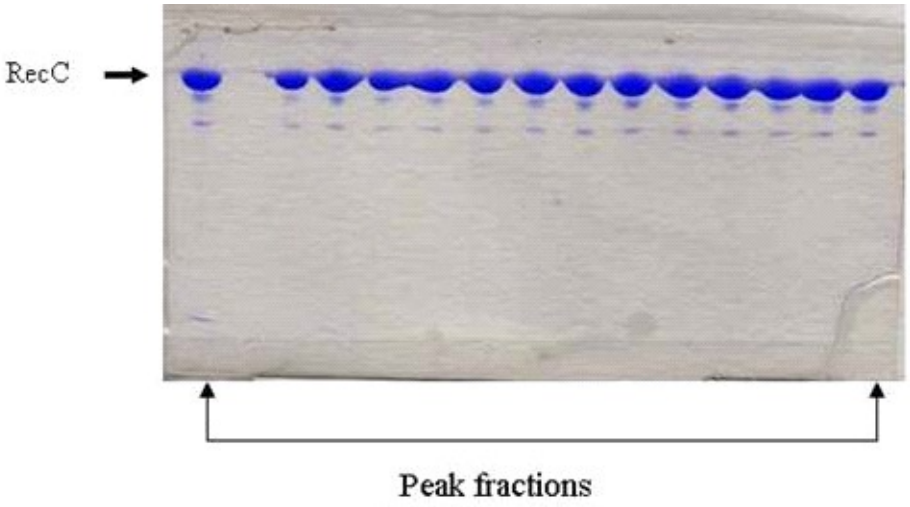

Figure 3.10: 12% SDS PAGE of RecC fractions from Hi-Trap heparin column.

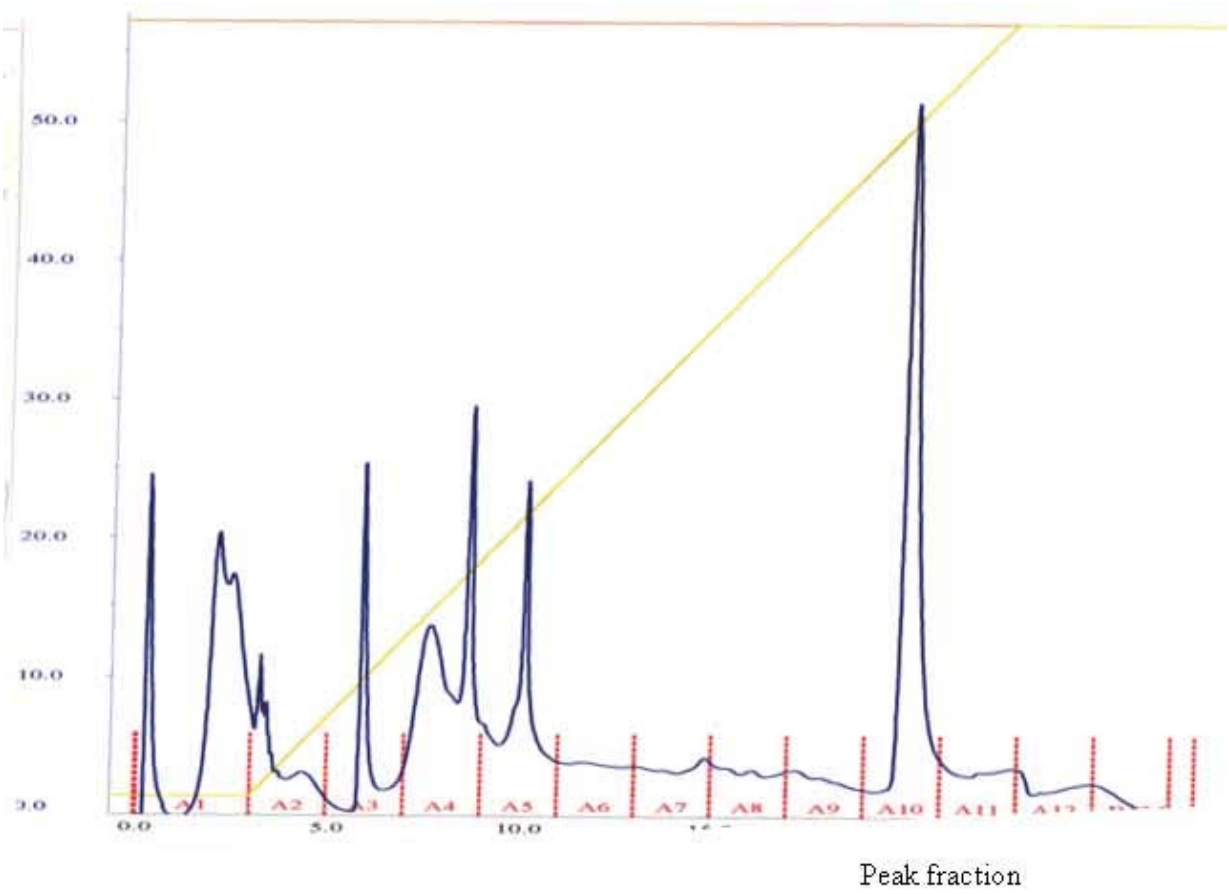

Figure 3.11: Elution profile of RecC from Hi-Trap MonoQ column. The protein elutes as a single peak which shows that it is pure. The red line, yellow line and blue line indicate flow-rate, gradient concentration and absorption at 280 nm respectively.

3.2.5 Co-purification of 100kDa-RecC complex

The M15 and V186 cells containing the plasmids for overexpressing the 100kDa and RecC respectively were grown separately and harvested together. The ratio of the culture volumes of the 100kDa and RecC were 2:3. The RecC was grown in larger culture volume because the V186 cells do not over express the protein as well as the M15 cells. The lysate of the pooled cultures of 100kDa and RecC were prepared by sonicating the cells as described in the materials section. The lysate was then treated with 40% ammonium sulfate to precipitate the complex of 100kDa and RecC. The precipitated complex was isolated as a pellet by centrifuging at 15000 rpm for 90min using a JA-20 rotor. The pellet was then re-dissolved in NBB and loaded on a nickel column. The 100kDa has a his-tag, hence, the complex was purified using a Hi-Trap chelating nickel column. The pooled peak fractions from the nickel column were then loaded on a Hi-Trap heparin column for further purification. The purification procedure used is described for the 100kDa. The peak fractions from the heparin column were pooled and run on a ss-DNA agarose column (Sigma) in presence of 20mM magnesium. The ss-DNA agarose column was used for further purification of the protein complex. The purity of the complex was checked by running a 12% SDS PAGE.

3.2.6 Fe-cleavage of the 100kDa domain

For the experiments presented here, the 100 kDa helicase domain of RecB was dialyzed against 40 mM Tris-HCl (pH 7.4) to equilibrate the enzyme for the cleavage reaction and to remove glycerol, which scavenges hydroxyl radicals and interferes with the Fenton chemistry. The enzyme solution was then concentrated using 4 ml Amicon Ultra-4 centrifugal devices. The centrifugation was carried out using a Beckmann Centrifuge with a JA-20 rotor at speeds of 5000 rpm. Ferrous sulfate (0-1000 μM) was added to 5- 100 μM enzyme in 40 mM Tris-HCl buffer, pH 7.4. The typical volume of the reaction mix was 20μl and it was incubated for 15 min on ice followed by the addition of sodium ascorbate (25 mM). The solution then sat on ice or at room temperature for an additional period of 30 min to 24 h. The Fe-cleavage reactions were stopped by adding 2mM EDTA. Also, the cleavage reactions were carried out under other conditions as described in detail in the results section.

3.2.7 Sodium Dodecyl Sulfate-Polyacrylamide Gel Electrophoresis.

12% SDS polyacrylamide gels and tricine-SDS polyacrylamide gels were run to visualize the small cleavage products from the cleavage reactions. Electrophoresis was carried out at 35 mA at room temperature for approximately 4 h. Gels were studied after they were de-stained with 50% methanol and 10% acetic acid. Benchmark pre-stained molecular mass markers obtained from Invitrogen were used to estimate the mass of the Fe^{2+}/ascorbate-generated protein cleavage fragments that had been run on SDS-polyacrylamide gels. The protein

bands were visualized by staining with 0.1% Coomassie Brilliant Blue in 50% acetic acid.

3.2.8 Inverse gradient gel:

Inverse gradient gels obtained from Gelux labs (699 Columbia Ave, Akron, OH 44310) were used to analyze the cleavage products from the 100kDa cleavage reaction. The gel had a gradient of 16-4% polacrylamide from the top to the bottom of the gel. The gradient of polyacrylamide helped to resolve the cleavage products better than 12% SDS PAGE. The running buffer contained Tris.HCl and Glycine. The buffer composition is listed in Table (3.1) The gels were Comassie stained as previously described.

3.2.9 RecB and RecC interactions studied by surface plasmon resonance

Biacore X instrument method is based on the optical phenomenon surface plasmon resonance (SPR). This technique essentially detects a change in refractive index (RI), when a molecule binds to another molecule immobilized on a surface such as gold. A molecule (in our case a protein) is immobilized on the surface by using a chemical coupling reaction. After immobilization, a second protein molecule is passed over the surface. The interaction between these protein molecules is captured by a change in the refractive index which can be visualized in real time as a plot between time and refractive index (RI)/ response difference.

Biacore X in Dr. Peter Schuck's laboratory at NIH was used for the experiments to study the binding between the RecB and RecC subunits. The sensor chip used was made of dextran matrix. The sensor surface was activated by adding 60 µl of NHS (N-hydroxysuccinimide) and EDC (N-ethyl-N'-(3-dimethyl aminopropyl)-carbodiimide hydrochloride). Amine coupling chemistry (direct linkage via primary amines on the protein/peptide) helps the activated sensor surface to couple with the protein molecule. In the experiments discussed in this chapter the RecC was coupled or immobilized on the sensor surface and the binding change upon the addition of RecB by injection was observed. Both RecC and RecB were dialyzed in 10 mM acetate buffer (pH = 4). The concentrations of both the subunits were in the µM range. The flow rate during the binding was 3 µl/min. At all other times during washes and surface activation/deactivation the flow rate was 5 µl/min. The running buffer was 0.01M HEPES (pH=7.4). Binding changes between RecB and RecC were studied in the presence and absence of magnesium. After each run (to measure the binding of RecB and RecC) the surface was deactivated by injecting 30 µl ethanolamine and reactivated by NHS/EDC before the next run.

3.2.10 ss-DNA agarose column chromatography

Method 1: Individually purified RecC and 100kDa were mixed and loaded and eluted from a gravity flow ss-DNA agarose column. Purified 100kDa and RecC were combined in 1:1 ratio in and incubated on ice for 1-2 hours in Buffer D. The

protein mixture was then loaded on two different 5 ml ss-DNA agarose column. One column was washed and eluted with BufferD containing 20mM $MgCl_2$ and the other was eluted with Buffer D without $MgCl_2$ (Table 3.1). Elution was done by applying a gradient of 0-1M NaCl. The wash and elution fractions that were collected had a volume of 1ml each. The fractions were analyzed on a 12% SDS PAGE gel.

Method 2: The RecC subunit and the 100kDa helicase domain of RecB were copurified as described in the materials section. This purification procedure using the nickel column showed that even in the absence of magnesium, the 100kDa and RecC form a complex and coelute in the elution fractions. In the next step we used ss-DNA agarose column to see if the presence of ss-DNA and magnesium altered this interaction. The copurified 100kDa and RecC were then loaded on two ss-DNA agarose columns. The columns were washed and eluted as described in Method 1 in absence and presence of 20 mM $MgCl_2$. The wash and elution fractions were then analyzed on a 12% SDS PAGE.

3.2.11 Spin column experiments:

The 100 kDa is histidine tagged and it was bound on spin columns containing a chelating metal like nickel or cobalt. The effect of magnesium on the complex formation between 100kDa and RecC was studied using spin columns by complexing 100kDa and RecC in a ratio of 1:1. This ratio was based on concentrations which were calculated based on absorbances at A_{280}. The Nickel-NTA spin columns obtained from Qiagen were pre-charged with nickel, whereas the spin columns from Pierce had to be charged with a cobalt containing resin.

The spin columns required a protein concentration of 100-150µg .Both the proteins were dialyzed in a buffer containing 20mM $NaPO_4$, 50mM NaCl, 1mM EDTA and 0.1mM DTT (pH=7.8). The buffers used for binding (NBB) and eluting (NEB + 1M Imidazole) the complexed 100kDa and RecC contained 20mM $MgCl_2$ for the column that was used to study the effect of magnesium. In the control set the buffers used for binding and eluting of the complexed 100kDa and RecC did not contain magnesium. The binding of the 100kDa to the chelating spin columns was done by incubating the protein in NBB (pH=7.8) column for 1-3 hrs on ice. Unbound 100kDa was spun out by centrifuging at 2Xg in an Eppendorf centrifuge. RecC was then added to the column containing the bound 100kDa and incubated for another 1 hour. Any unbound complex was spun out of the column by centrifugation. The column was then eluted with 50µl NBB and NEB. The flow-through from the washes with NBB and NEB were collected and run on a12% SDS PAGE.

3.2.12 Gel Filtration

Calibration of the Superose-6 column:

The 24ml Superpose-6 column was calibrated using Bio Rad and Sigma Gel Filtration standards with molecular weight ranges between 29,000 – 669,000

The Bio-Rad standard was used to estimate the void volume of the column which was found to be approximately 7.5 ml which is in close agreement with the void volume supplied by the company (Void volume (V_o) = 30% of

column volume = 30% of 24ml = 7.2ml). The FPLC trace of the column calibration using Bio-Rad standard is shown in figure (3.12).

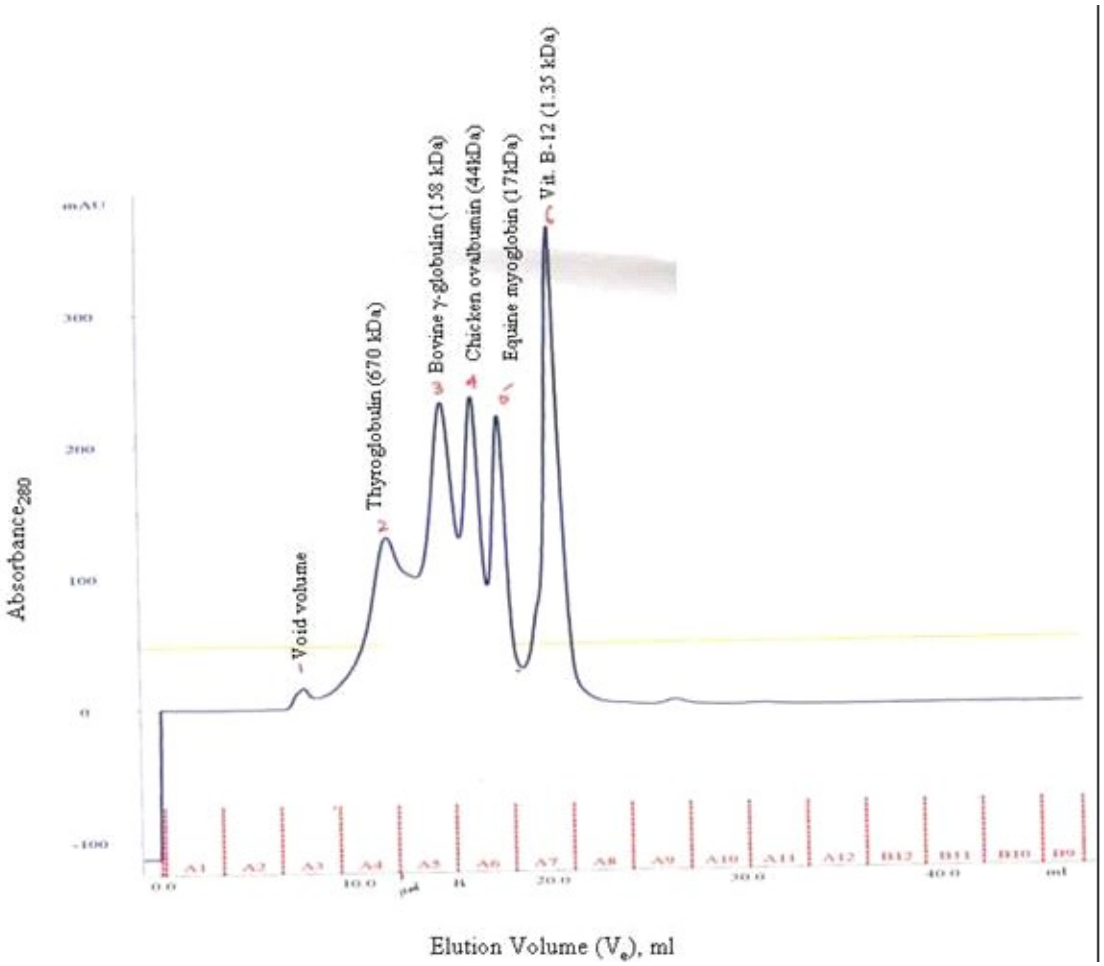

Figure 3.12: Calibration of Superose 6 column with Bio Rad Standard.

3.2.13 Mass-Spectrometry:

The samples for mass-spectrometry were prepared by dissolving them in trifluroacetic acid using a C4 ziptip. A shimadzu mass-spectrometer was used. MALDI-TOF technique was used to obtain the spectra of the samples of the Fe-cleavage reactions. The spectra was obtained with the help of Noel Whittaker at the mass-spectrometry facility in the Department of Chemistry and Biochemistry, University of Maryland, College Park.

3.3 RESULTS:

3.3.1 Effect of Mg^{2+} on the Interactions of RecB, 100kDa and RecC

The effect of magnesium on the interactions of the RecB, 100kDa fragment of RecB and the RecC subunit were studied using multiple techniques. In this section I will discuss the techniques and the results obtained from these experiments.

3.3.1.1 Biacore X Binding Experiments

The binding and dissociation profile of the full length RecB and RecC subunits were studied using Biacore X. These set of experiments were a part of an initial study to see if magnesium had any effect on the binding of the RecB and RecC subunits. In our experiments RecC was immobilized on the surface by amine coupling chemistry and RecB was passed over this surface. The RecB used for most of these experiments was from a stock in our laboratory. The experiments were carried out as described in the materials section of this chapter. Unbound RecC was washed away by passing the running buffer over the surface. Immobilization of RecC was detected by observing a change in the RI as shown in Figure (3.13). A change in the response difference signal (marked change in refractive index) was observed which indicated binding. The signal decreased slowly when the running buffer was passed through the chip and this indicated slow dissociation. In the presence of 20mM Mg^{2+}, a stronger binding signal was observed. In presence of 1M NaCl and EDTA a rapid dissociation was observed because the EDTA chelated the magnesium ions, thus weakening the binding

between the RecB and RecC subunits (Figure 3.13 & 3.14). These results indicated that Mg^{2+}enhances the interaction between RecC and RecB. The prime difficulty faced with this technique was that RecB was difficult to purify in very large and pure amounts. Also RecB was not very stable over long periods of time.

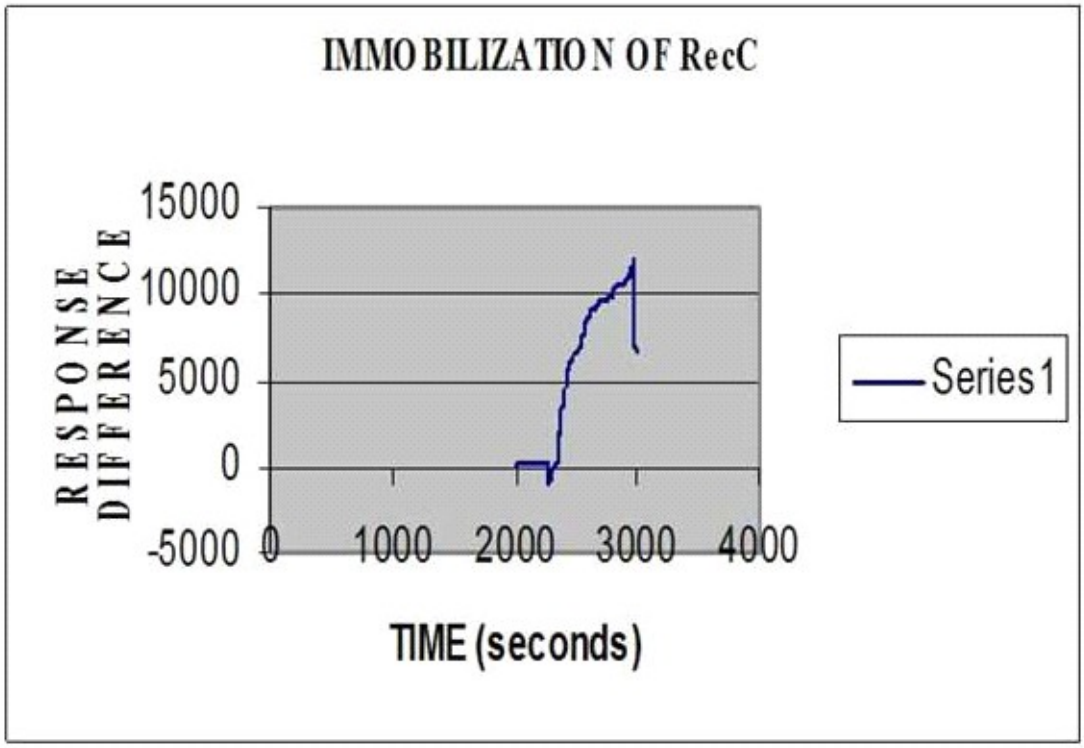

Figure 3.13: Plot of RI (response difference) and time. This plot shows the immobilization of RecC on the surface. The increase in RI indicated immobilization of RecC. The drop in the RI indicates the washing away of unbound RecC.

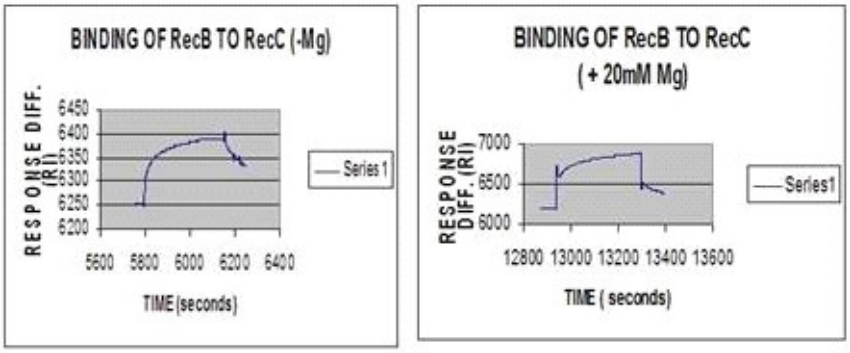

Figure 3.14: Difference in binding interactions between RecB and RecC in presence or absence of magnesium. The figure on the right and left shows the response difference after the binding of RecB and RecC in the absence or presence of magnesium respectively. The increase in RI is 1000 units in presence of magnesium as compared to an increase in 200 units in the absence of magnesium. This indicates that magnesium enhances the binding of RecB and RecC.

3.3.1.2 ss-DNA agarose column chromatography

The Biacore results indicated that there is an effect of magnesium on the interactions of the RecB and RecC subunits. At this point we decided to work with the 100kDa helicase domain of the RecB subunit because preliminary work done previously in our laboratory by Dr. Olga Carlson indicated that magnesium in the presence of DNA enhanced the binding of the 100kDa and RecC (Figure 3.2). The 100kDa was stable and easier to purify in large amounts than full length RecB. Moreover, the 100kDa is a helicase and had requirements for magnesium. Also, the recently solved crystal structure of RecBCD showed that the 2B domain of RecB which is located in the 100kDa helicase domain was a contact point with RecC. The effect of magnesium on the binding of RecC and the 100kDa helicase domain in the presence of ss-DNA was studied using ss-DNA agarose columns from Sigma. This experiment was performed in two different ways as described in the materials section.

Method 1: Individually purified RecC and 100kDa were mixed and loaded and eluted from a gravity flow ss-DNA agarose column. The results obtained from Method 1 show that most of the RecC was in the flow through of the wash fraction of the ss-DNA column that was eluted without $MgCl_2$ compared to the column that was eluted with 20mM $MgCl_2$. This observation strongly illustrates that magnesium enhances the binding of 100kDa and RecC.

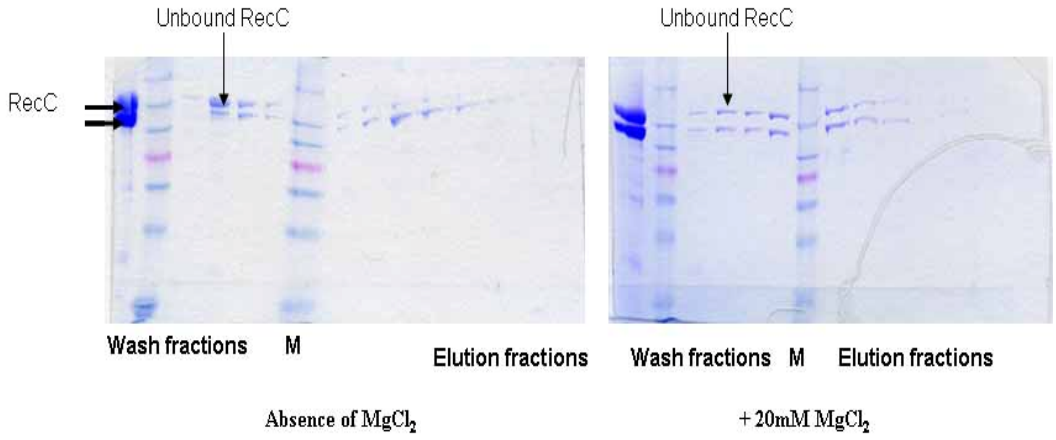

Figure 3.15: ssDNA-agarose column fractions of 100kDa-RecC complex in the absence and presence of 20mM of magnesium.

Method 2: The RecC subunit and the 100kDa helicase domain of RecB were copurified on a nickel column (Figure 3.16). The purified complex of the 100kDa and RecC were then and loaded on a ssDNA agarose column. In presence of 20mM $MgCl_2$ the 100kDa and RecC coeluted during the gradient elution as compared to in absence of $MgCl_2$ (Figure 3.17). This shows that the presence of magnesium and DNA enhances the formation of complex between the 100kDa and RecC. This method is described in the materials section.

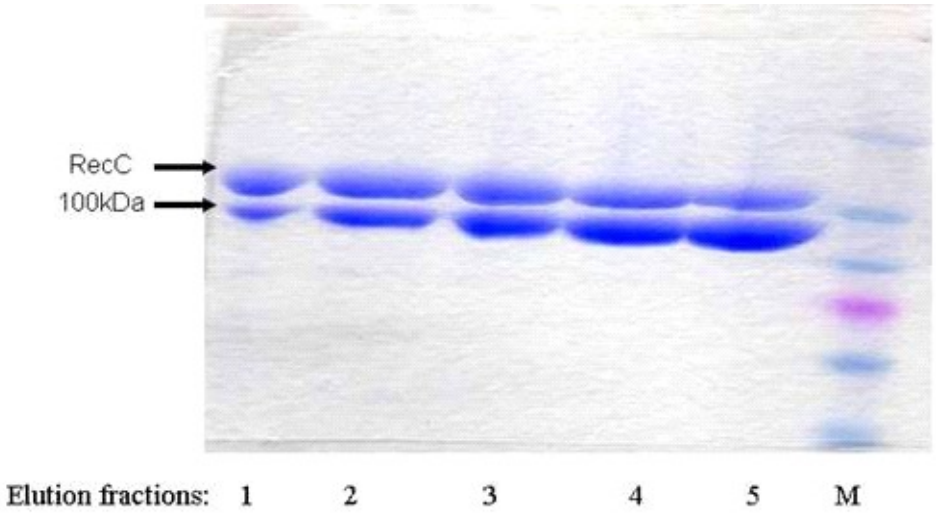

Figure 3.16: Peak fractions of Complexed 100kDa and RecC from the nickel column.

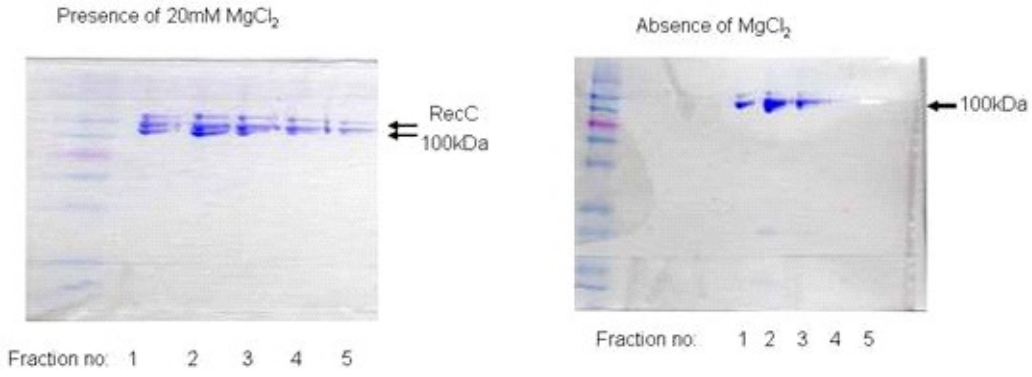

Figure 3.17: Elution fractions of complexed 100kDa and RecC from the ssDNA agarose column.

3.3.1.3 100kDa and RecC interactions studied using nickel and cobalt spin columns

The RecC alone did not bind to the chelating columns and this was confirmed by incubating just RecC in the column and spinning the column to collect the flow-through. The flow-through was analyzed on a 12% SDS gel and it was found that the RecC was in the flow through.

Binding of 100kDa to RecC in presence or absence of magnesium was studied in parallel by using two spin columns.

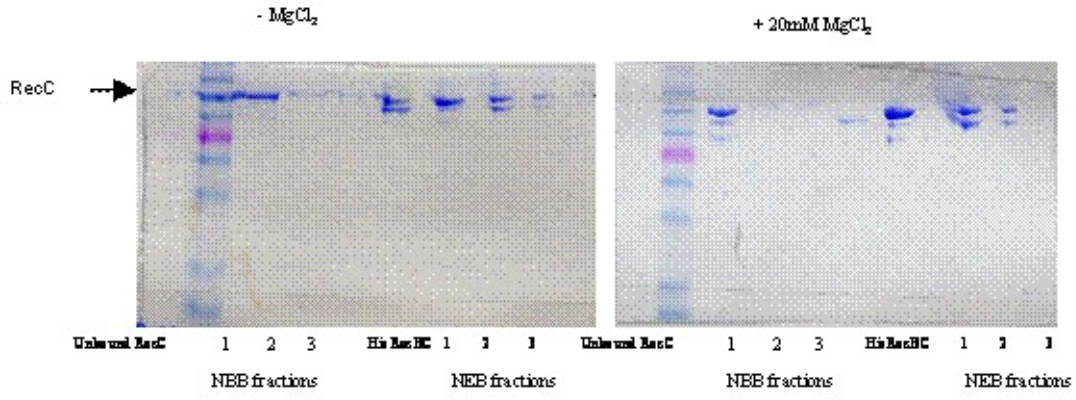

Figure 3.18: Spin column fractions of the binding experiments between 100kDa and RecC.

The gel shows that there is unbound RecC present in the first lane of the gel in absence of $MgCl_2$ as compared to the gel in presence of 20mM $MgCl_2$ 9(Figure 3.18). This indicates that RecC forms a strong complex with 100kDa in the presence of magnesium. Also, the fractions from the NBB contained unbound RecC in absence of magnesium as compared to in presence of 20mM magnesium. The NEB fractions in the gel in the presence of 20mM magnesium contained more complexed 100kDa and RecC as compared to the gel in the absence of magnesium. This is very clear in the lane containing Fraction 1 of NEB. These results again corroborate the fact that the binding of 100kDa and RecC is enhanced in the presence of magnesium.

The ss-DNA agarose chromatography and the chelating spin column experiments show that the binding of the 100kDa and RecC is enhanced in presence of magnesium. This enhancement in binding is more pronounced when the interactions between the 100kDa and RecC are studied in presence of ss-DNA. This could be because the magnesium ions are required to shield the charges of the negatively charged ss-DNA strand. Moreover, the crystal structure also shows that the RecC subunit has three channels, two of which accommodate ss-DNA and the third interacts with the 100kDa C-terminal helicase domain of the RecB subunit.

3.3.1.4 Gel Filtration

In an effort to quantify the role of magnesium on the binding interactions between the 100kDa helicase domain of RecB and RecC we used gel filtration. Gel filtration is a technique that is used to understand the size and shapes of protein molecules. It separates protein molecules based on their size and shapes. A larger protein molecule will flow through the spaces between the gels as it cannot fit into the pores of the gel matrix and elute out early as compared to an smaller protein molecule which will wind its way through the pores of the gel matrix and elute later. We used gel filtration to study the complex of 100kDa and RecC in presence or absence of magnesium to get an idea of the behavior of the complex. The purified complex was run through a Superose 6-HR-10/30 column (Amersham) at different concentrations of magnesium. The elution volume was recorded and it was used to calculate the apparent molecular weight according to the following equation.

$K_{av} = (V_e - V_o) / (V_t - V_o)$

Where K_{av} = Binding constant which is linearly related to the logarithm of molecular weight of the protein complex.

V_e = Elution volume of the protein

V_o = Column void volume

V_t = Total elution volume.

If the complex is compact in shape it will elute later and thus, have a larger elution volume V_e

The Superose 6 column was then calibrated as described in the materials section with Sigma molecular weight standards and a standard plot of V_e/V_o versus log mol.wt. was obtained (Figure 3.19). This plot was then used to forecast the molecular weights of the 100kDa-RecC complex under different concentrations of magnesium.

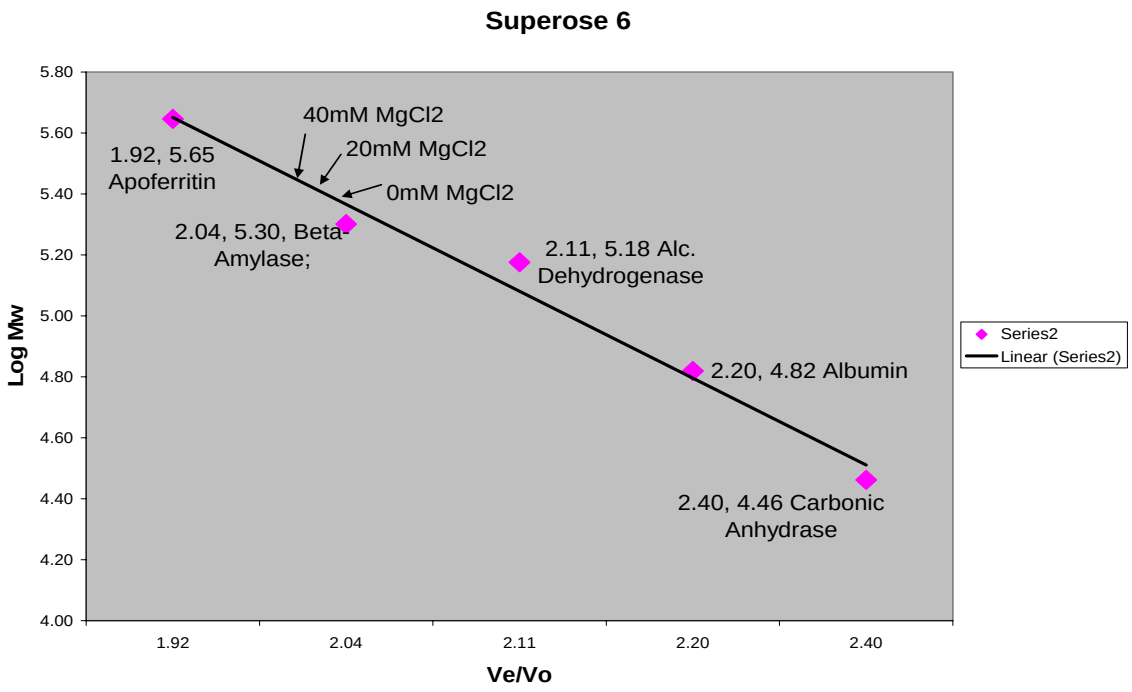

Figure 3.19: Standard curve for Superose 6 column for estimating the apparent molecular weight. The arrows indicate the elution positions of the 100 kDa -RecC complex in presence of 0 mM, 20 mM and 40 mM $MgCl_2$.

The molecular weights of purified 100kDa-RecC complex were determined in the absence and presence of different concentrations of magnesium. The complex was formed by copurifying the 100kDa and RecC. The concentrations of the complex used for the gel filtration experiments ranged from 0.1-0.5 μM. The running buffer used for these experiments contained 50mM Tris.HCl, 0.15M NaCl + 1mM DTT. In the runs without magnesium, 1mM EDTA was added to the running buffer. The column was eluted with two column volumes and equal fractions of 1ml were collected. These peak fractions were then concentrated using a 5ml Amicon centrifugal filter and analyzed on a 12% SDS PAGE to confirm that the protein eluting at the particular elution volume (V_e) was the complex of 100kDa and RecC. The elution volume was determined from the centre of the peak fractions. The apparent molecular weights of the 100kDa-RecC complex at different magnesium concentrations are tabulated in Table 3.2.

Conc. of Mg2+(mM)	Ve [Elution vol.](ml)	Ve/Vo	Mol.wt. of complex(kDa)
0	14.6	2.03	217
20	14.4	1.99	267
40	14.3	1.98	281

Table 3.2: Dependence of apparent molecular weight of the 100kDa-RecC complex on the concentration of $MgCl_2$.

The apparent molecular weight of the 100kDa-RecC complex increases with increasing concentrations of magnesium. This indicates that the shape of the complex may be less compact in the presence of magnesium and elutes out of the column at much lower elution volumes (V_e). Also, the elution volumes obtained for these experiments were well within the range of the elution volumes of the standard plot that was used to forecast the values of the molecular weights. The molecular weights obtained were in good agreement with theoretical values. The experiments were repeated, but the molecular weights obtained were not the same every time but they were in a reasonable range. This experiment showed that magnesium probably enhanced the binding of RecC and 100kDa. However since the difference in elution volumes were small the effect of magnesium cannot be quantitatively estimated.

3.3.2 Mapping of Magnesium Binding sites in the 100kDa Helicase Domain of Rec B

The 100kDa domain is a helicase domain and is also a major point of contact with RecC. Thus, it is plausible that the 100kDa domain had sites for magnesium binding. Fenton chemistry was used to study if there was any magnesium binding sites in the 100kDa helicase domain.

3.3.2.1 Fe-cleavage of 100kDa helicase domain of RecB

The magnesium metal binding sites in 100kDa were studied using Fenton chemistry. The Fe- cleavage conditions were first optimized with extensive experimentation. It was much harder to optimize the cleavage conditions for the 100kDa domain as it was a much larger protein than the 30kDa nuclease domain of RecB. The Fe-cleavage reactions with the 100kDa yielded two distinct cleavage products. The two cleavage products had a molecular mass in the range of 60 – 80 kDa. In this section, the optimization of the cleavage reactions that yielded two distinct cleavage products when the 100kDa domain was treated with ferrous ions is discussed. The yield of the cleavage products was not as high as the cleavage products obtained from the 30 kDa nuclease domain. Hence, the cleavage products were not visible on the gels if they were coomassie stained and the gels had to be silver stained to visualize the cleavage products. After several sets of experiments, we were able to find a set of conditions at which the cleavage products could be visualized in a reproducible manner. The standardized set of conditions was then used to obtain further data.

3.3.2.2 Fe-cleavage at different enzyme concentrations

Cleavage reactions were carried out at different enzyme concentrations to find out the optimal amount of enzyme required to obtain the cleavage products if any which could then be visualized. The reactions were carried out as described in the materials section. The reactions conditions are summarized below in Figure (3.20). From these experiments it was found that the enzyme concentration should be at least 0.5μM to visualize the cleavage products by silver staining. Also, the cleavage products could not be visualized by silver staining at higher enzyme concentrations of 2μM as it resulted in a lot of background.

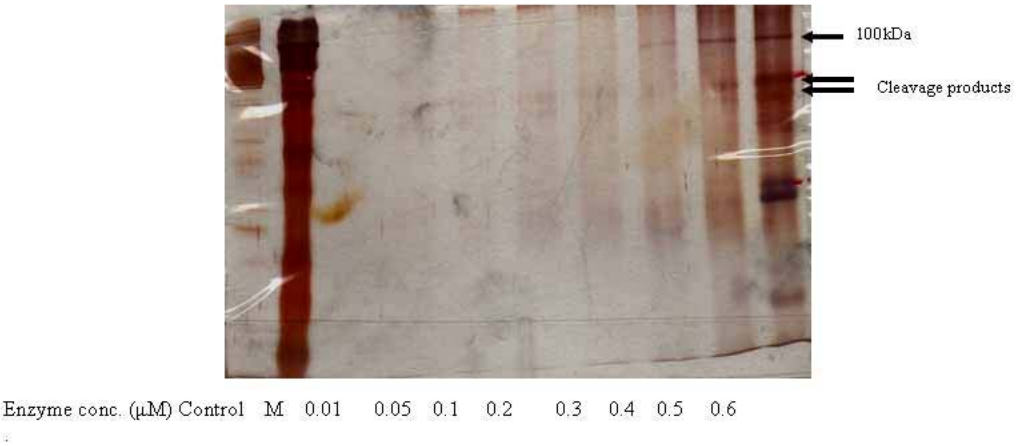

Figure 3.20: Fe-cleavage of 100kDa at different enzyme concentrations, 1mM $FeSO_4$, 25mM Na-ascorbate, 40mm Tris.HCl (pH=7.4) at RT.

3.3.2.3 Fe- cleavage of 100kDa at different $FeSO_4$ concentration

Ferrous sulfate ($FeSO_4$) was used as the source of Fe^{2+} ions in the 100kDa Fe-cleavage reactions. Very high concentrations of ferrous ions caused extensive cleavage and degradation of the protein. Different concentrations of ferrous sulfate were included in the reaction mixture and the cleavage reactions were carried out. The reactions were carried out as described in the materials section. The cleaved products were visualized on a 12% SDS gel by silver staining (Figure 3.21). From several sets of experiments it was found that the optimal ferrous ion concentrations that were required for optimal cleavage of the 100kDa were between 500μM – 1000μM (1mM). The cleavage products were visualized on a 12% gel by silver staining.

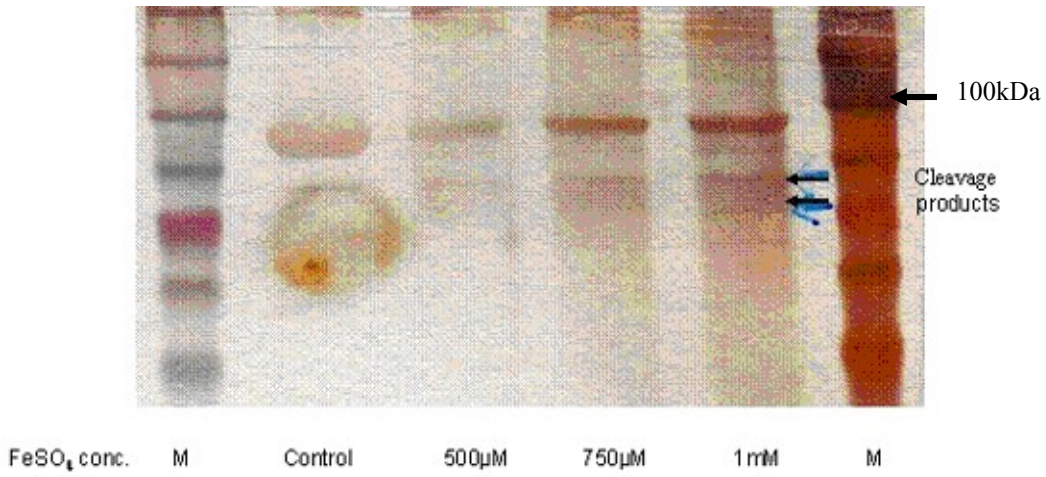

Figure 3.21: Fe-Cleavage of 100 kDa at different concentrations of $FeSO_4$, 1µM enzyme, 25mM Na-ascorbate, 40mM Tris.HCl (pH= 7.4) at RT. M stands for Marker.

3.3.2.4 Fe-cleavage of 100kDa at different incubation times

To optimize the incubation time that yielded distinct cleavage products the cleavage reactions were carried out for different time periods keeping the enzyme and $FeSO_4$ concentrations constant. The cleaved products were visualized on a 12% gel SDS PAGE by silver staining (Figure 3.22). From the experiments it was found that an incubation time of 1- 1.5 hours yielded the optimal amount of cleavage products. Incubation times below or above this range yielded too little or too much degradation products. The reaction was performed as described in the materials section.

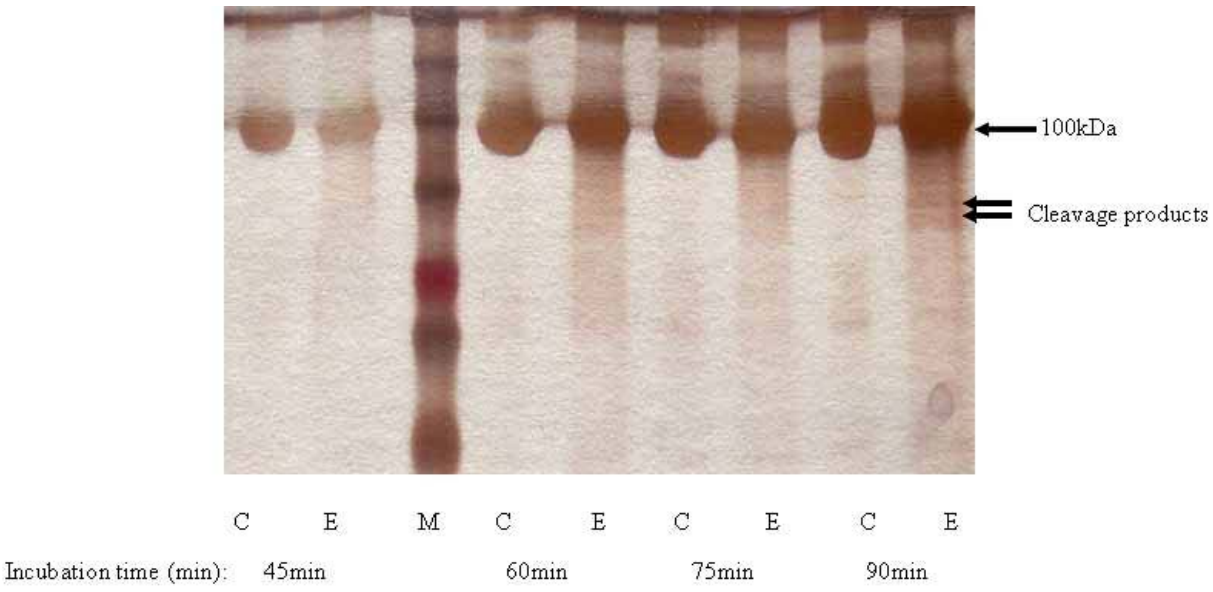

Figure 3.22: Fe-cleavage of 100 Da at different incubation times, 1μM enzyme, 1mM $FeSO_4$, 25mM Na-ascorbate, 40mM Tris (pH=7.4) at RT. C stands for control, E stands for experimental and M stands for Marker.

3.3.2.5 Fe-cleavage reactions with 100kDa and cross-linking

During the above Fe- cleavage experiments with the 100kDa a high molecular weight product was obtained when the protein was treated with ferrous ions. This high molecular weight product was obtained possibly because of cross-linking of the tyrosine residues in the protein molecules in presence of transition metals like iron. Similar products were obtained with proteins like ribonuclease A were treated with nickel. The cross-linking was due to the formation of a dityrosine and the inclusion of excess tyrosine in the reaction inhibited the formation of such cross-linked protein dimer. The excess included tyrosine instead formed a protein-tyrosine cross-link (54). In an effort to see if the formation of the cross-linked products could be inhibited in our cleavage reactions with ferrous ions we added tyrosine to the reaction mix of the Fe-cleavage reactions. The goal of including tyrosine was to see if the inhibition of such cross-links yielded better cleavage products. From our experiments we found that the inclusion of 1μM tyrosine did decrease the formation of cross-linked products to some extent but it did not improve the extent of protein cleavage. Also, the yield of the cleavage products was not affected by the inclusion of tyrosine in the reaction mix. The results are shown below in Figure (3.23).

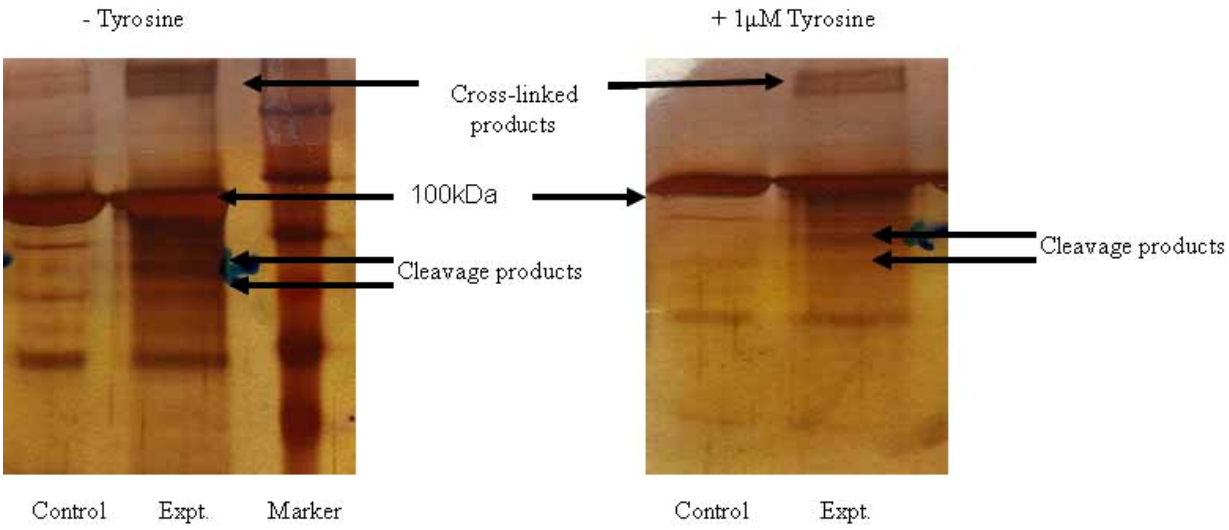

Figure 3.23: Fe-cleavage of 100 kDa in the absence and presence of tyrosine, 1μM enzyme, 1mM $FeSO_4$, 25mM Na-ascorbate, 40mM Tris.HCl (pH=7.4) at RT.

3.3.2.6 Fe-cleavage of 100 kDa in presence of hydrogen peroxide (H_2O_2)

Hydrogen peroxide was included in the Fe-cleavage reaction mix as a supplement to dissolved molecular oxygen. With the inclusion of peroxide we wanted to see if the reaction yielded better cleaved products in a shorter incubation time. The results from these experiments showed that inclusion of 2mM peroxide leads to the rapid degradation of the 100 kDa protein. The figures from these experiments are not shown. On the other hand inclusion of 2mM peroxide and 1μM tyrosine leads to a more controlled cleavage reaction. The reaction was incubated in presence of tyrosine for different time periods. After the incubation period 2mM peroxide was added and incubation was carried out for 1min before it was quenched with EDTA. The result from this experiment is shown in the figure below (Figure 3.24).

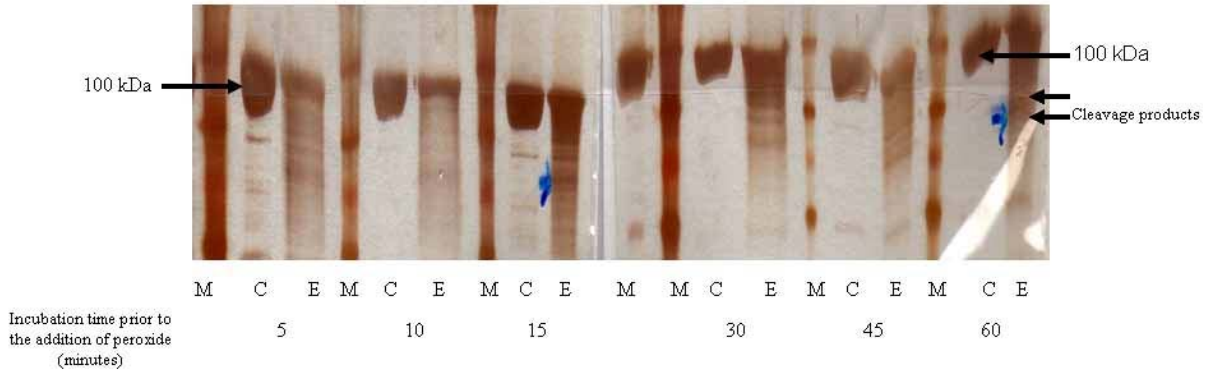

Figure 3.24: Fe-cleavage of 100kDa in presence of 2mM H_2O_2 and 1μM tyrosine, 1μM enzyme, 1mM $FeSO_4$, 25mM Na-ascorbate, 40mM Tris.HCl (pH=7.4) at RT. C stands for control and E stands for experimental sets. M stands for Marker.

3.3.2.7 Optimized conditions for the Fe-cleavage of 100kDa

The multiple sets of experiments under different conditions (~ 800-1000) were done and the representative results were presented in the previous section. From these experiments it was found that a unique cleavage product was obtained when the 100kDa protein was treated with 1mM $FeSO_4$, 25mM NaAsc in the presence of 40mM Tris buffer (pH=7.4) for 1 hour at room temperature (RT). In the latter part of this project we attempted to sequence the cleavage products. In order to do so we had carried out the cleavage reactions under the optimized conditions at high concentrations of the enzyme and visualized the cleaved products on a SDS PAGE by coomassie staining.

3.3.2.8 Fe-cleavage of 100kDa with optimized conditions at high enzyme concentrations

The Fe-cleavage reactions were carried out at high enzyme concentrations with the optimized conditions. The cleavage products were visualized on a 12% SDS PAGE. The cleaved products were visible at high enzyme concentrations but they were not very well resolved. The figures below is a representative gel that shows the reproducibility of the 100kDa Fe-cleavage reactions at higher enzyme concentrations (Figure 3.25). Moreover, the cleavage reactions were also carried out at different temperatures and the results obtained indicate that the room temperature (RT) is the optimal temperature for the cleavage reactions to occur (Figure 3.26).

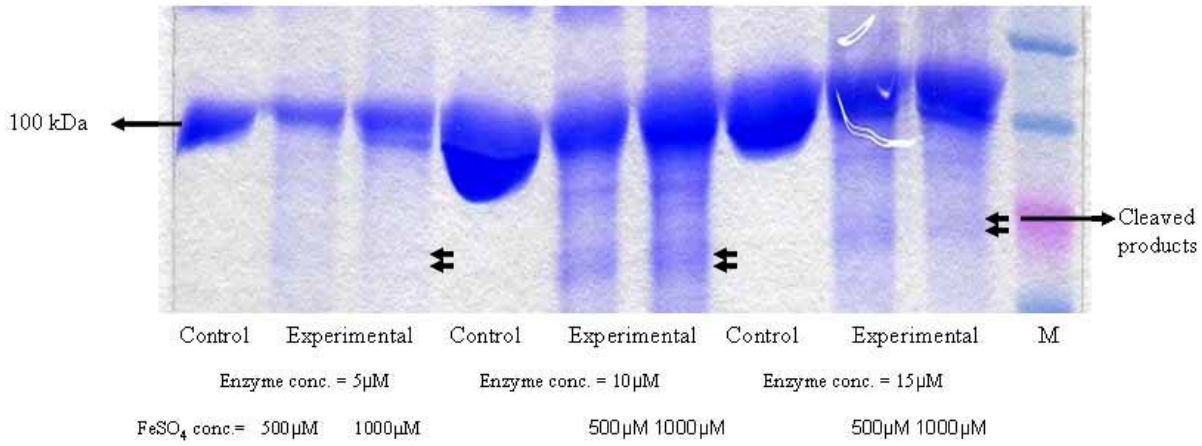

Figure 3.25: 12% SDS PAGE of Fe-cleavage of 100 kDa after optimization of the reaction conditions. Cleavage reactions were carried out at different enzyme and $FeSO_4$ concentration, 25mM Na-ascorbate, 40mM Tris.HCl (pH=7.4). The cleavage products are indicated by double arrows.

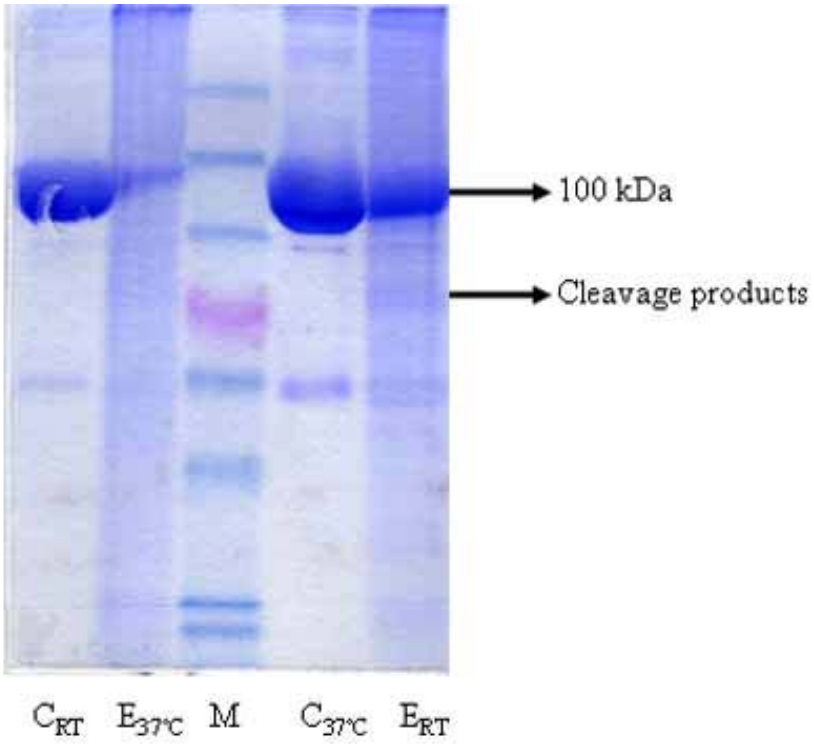

Figure 3.26: 12% SDS PAGE of 100kDa Fe-cleavage at different temperatures. Reactions were carried out in the presence of 10μM enzyme, 1mM $FeSO_4$, 25mM Na-ascorbate, 40mM Tris.HCl (pH=7.4). C stands for control and E stands for experimental sets.

3.3.2.9 Fe-cleavage of 100kDa as visualized on an inverse gradient gel

The cleavage products could not be resolved well on a 12% SDS gel so we used an inverse gradient gel in Tris glycine buffer with 14-6% gradient to visualize the cleavage products. The higher percentage on the top of the gel helped in retarding the progression of the two products which had similar molecular weight. The products were well resolved on this gel and they were submitted for sequencing after transferring them to a membrane (Figure 3.27).

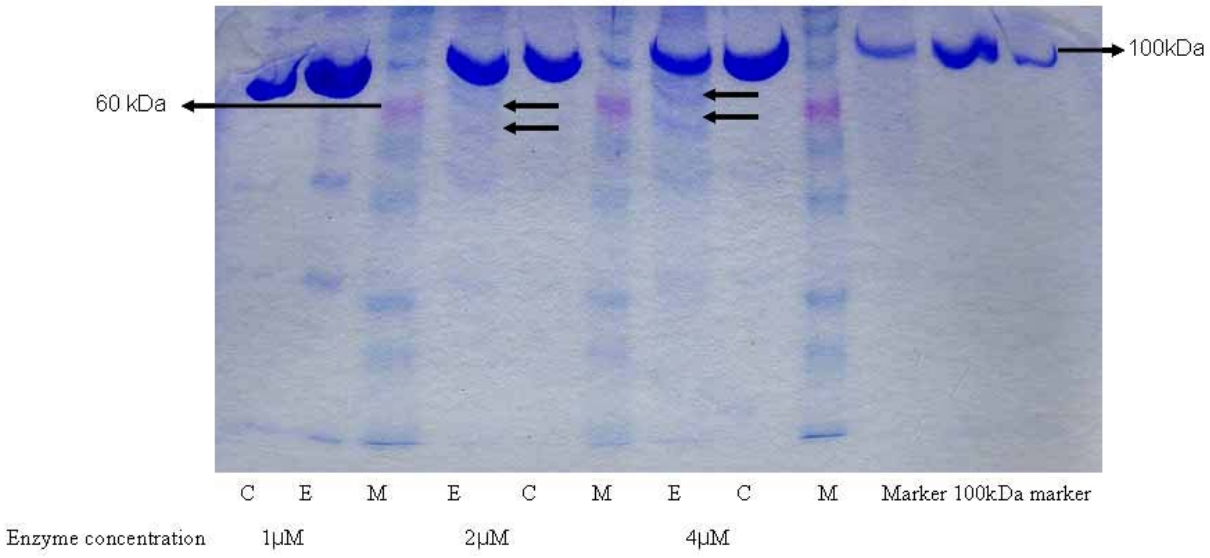

Figure 3.27: Inverse gradient SDS PAGE of Fe-cleavage of 100 kDa. Cleavage reactions were carried out at different enzyme concentration 1mM $FeSO_4$, 25mM Na-ascorbate, 40mM Tris.HCl (pH=7.4). The cleavage products are indicated by double arrows.

3.3.2.10 Sequencing of cleavage products

We tried to sequence the cleavage products of the 100kDa by Edman sequencing as described in the materials section. However, we were unable to obtain any sequence. The inability to obtain sequence information could have been due to various reasons. One of them was that the cleavage products were very large in size and their yield was low. The other reason could be that the side-chains of the cleavage products were reacting with the reactive oxygen-species giving rise to blocked N-terminals which could not be sequenced. So, we used mass spectrometry to get some insight into the sequence of the cleaved products. The method used for the MALDI-TOF mass spectrometry is described in detail in the materials section. We were able to detect the presence of the cleaved products in the reactions where the 100kDa protein was treated with Fe/Ascorbate as compared to control reactions in the absence of Fe/Ascorbate. The figures below shows the results obtained from the MALDI-TOF mass-spectrometry (Figure 3.28 & 3.29).

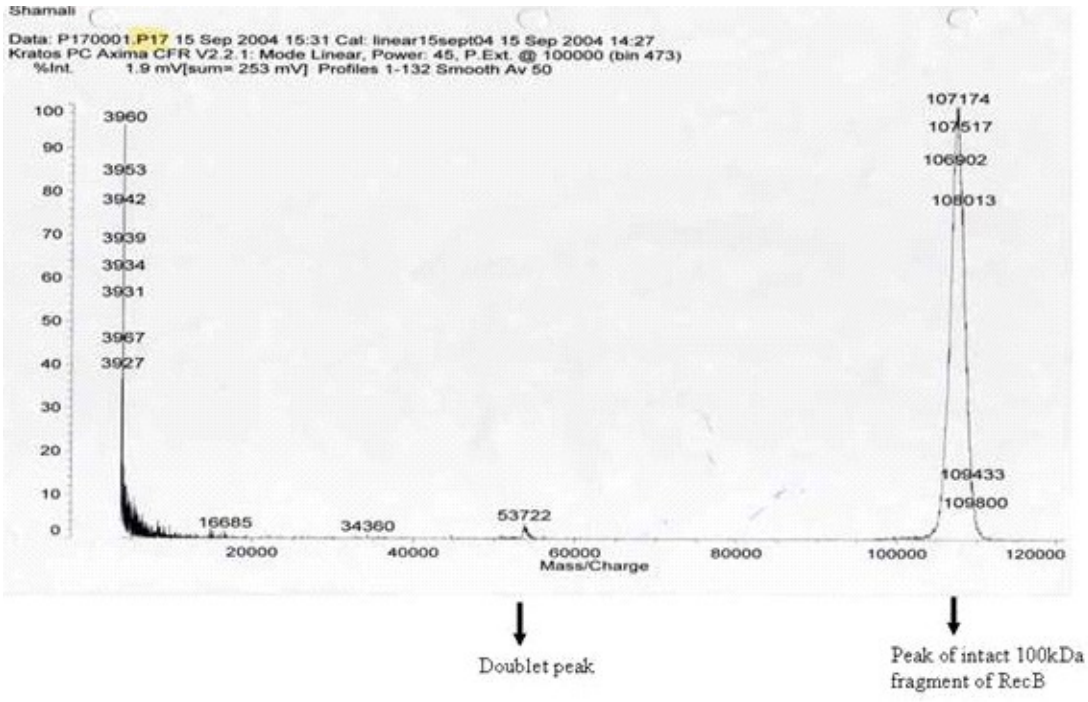

Figure 3.28: Mass Spectrogram of control 100kDa fragment of RecB(Not treated with Fe/ascorbate). The cleavage products are absent in the 60000-80000 region of the spectrum

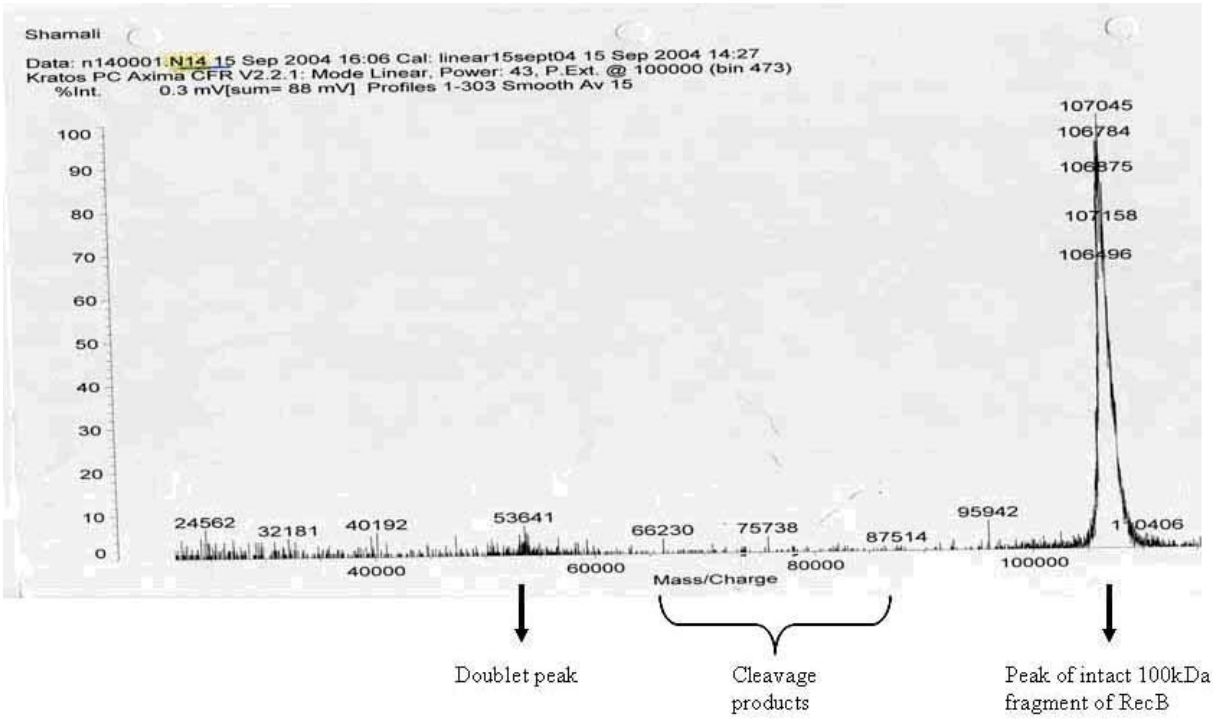

Figure 3.29: Mass-spectrogram of 100kda fragment of RecB treated with Fe/ascorbate. The cleavage products are present in the 60000-80000 region of the spectrum.

3.4 DISCUSSION

The role of magnesium is difficult to study because it does not bind tightly to the protein and is also present at fairly high intracellular concentrations, thus, making it difficult to study its role quantitatively. A combination of experimental approaches was used to provide some insight into the role of magnesium in the functioning of the RecBCD enzyme. Since, RecBCD is a DNA repair enzyme with helicase and nuclease activity magnesium is required to shield the negative charges of the DNA and it is also required for the helicase activity. Apart from this magnesium is also required in the stabilization of this large 330 kDa protein complex. The Biacore experiments showed the role of magnesium in complex formation between the 100kDa and RecC. In presence of magnesium the binding between the 100kDa and the RecC was enhanced. This indicates that magnesium is helping in the stabilization of the protein complex by binding in the interface of the two proteins. However, the complex was composed of the 100kDa fragment of the RecB subunit and RecC, hence to gain more complete insight into the role of magnesium in the interactions of the subunits it will be good to study the interaction of the full-length RecB and RecC. This kind of study has some intrinsic difficulties as it is difficult to purify the intact full length RecB in large quantities. The results of the experiments from the ss-DNA agarose column showed that the effect of magnesium in complex formation between the 100kDa and the RecC was more pronounced in the presence of ss-stranded DNA. Magnesium was required for the complex of 100kDa and RecC to be intact in the presence of ss-DNA.

We tried to quantify the role of magnesium in the complexation of the 100kDa and RecC by gel filtration studies but it was difficult to do so because magnesium is present at fairly high intracellular concentrations. The gel filtration experiments showed that the molecular weight of the complex in presence of magnesium was very close to the predicted theoretical molecular weight of the complex of 100kDa and RecC.

After gaining some insight into the role of magnesium in the complexation of 100kDa and RecC it was necessary to identify the binding sites of the magnesium metal in 100kda the helicase domain of RecB. Magnesium is required in DNA unwinding by the helicase domain and it is possible that it has a binding site in the helicase domain. The Fenton chemistry technique had helped us to identify the magnesium binding site in the 30kDa nuclease domain of RecB and we transferred this technique to identify the magnesium binding site in the 100kDa subunit of the RecB protein. We met with some success in doing so, as we were able to observe two distinct cleavage products. The formation of these two cleavage products in the presence of Fe/ascorbate indicates that magnesium has a binding site in the 100kDa helicase fragment of RecB. We were unable to obtain concrete binding sites as it was difficult to obtain a sequence for these cleaved products. The products were fairly large and also the cleavage products could have a blocked N-terminal. Moreover, it is possible that the reactive oxygen species formed during the Fe-cleavage experiments reacts with the protein side-chains and forms carbonyl derivatives (55). Such reaction products also make it harder to sequence the proteins. The results obtained for the Fe-cleavage

reactions showed that this technique is transferable to study the magnesium binding sites of proteins that require magnesium for its activities. However, it is difficult to apply this technique successfully to very large proteins like that of the 100kDa fragment of RecB. The work presented in this section to study the role of magnesium used multiple techniques and was exhaustive. However, detailed studies using Biacore, ultracentrifugation and light scattering experiments can be carried out to further study the role of magnesium.

.

Bibliography

1. Amundsen, S. K., Taylor, A. F., Chaudhury, A. M., and Smith, G. R. (1986) *Proc. Natl. Acad. Sci. USA* **83**, 5558-5562
2. Kowalczykowski, S. C. (2000) *Trends Biochem. Sci.* **25**, 156-165
3. Kowalczykowski, S. C. (1994) *Experientia* **50**, 204-215
4. Clark, A. J., and Sandler, S. J. (1994) *Crit. Rev. Microbiol.* **20**, 125-142
5. Marie Seigneur, S. D. E., and Bénédicte Michel. (October 1999) *Journal of Bacteriology,* **Vol. 181**, p. 6220-6221,
6. Kowalczykowski, S. C., Dixon, D. A., Eggleston, A. K., Lauder, S. D., and Rehrauer, W. M. (1994) *Microbiol. Rev.* **58**, 401-465
7. Wright, M., Buttin, G., and Hurwitz, J. (1971) *J. Biol. Chem.* **246**, 6543-6555
8. Kuzminov, A. (1999) *Microbiol. Mol. Biol. Rev.* **63**, 751-813
9. West, S. (1996) *Cell* **86(2):**, 177-180.
10. SC, W. (1996) *J. Bacteriol.* **8(5): 1**, 1237-1241
11. Taylor, A. F., and Smith, G. R. (1995) *J. Biol. Chem.* **270**, 24451-24458
12. Lieberman, R. P., and Oishi, M. (1974) *Proc. Natl. Acad. Sci. USA* **71**, 4816-4820
13. Finch, P. W., Wilson, R. E., Brown, K., Hickson, I. D., Tomkinson, A. E., and Emmerson, P. T. (1986) *Nucl. Acids Res.* **14**, 4437-4451
14. Taylor, A. F. (1998) *American Society for microbiology.)*, 231-263,
15. Smith, G. R., and Stahl, F. W. (1985) *BioEssays* **2**, 244-249
16. Willets, N., and Clark, A. (1969) *J.Bacteriol* **100**, 231-248
17. Emmerson, P. T. (1968) *Genetics* **60**, 19-
18. Capaldo-Kimball, F., and Barbour, S. (1971) *J. Bacteriol.* **106(1)**, 204-212
19. Chaudhury, A. M., and Smith, G. R. (1984) *J. Bacteriol.* **160**, 788-791
20. Clark, A. (1973) *Annu Rev Genet*, 67-86
21. Goldmark, P. J., and Linn, S. (1972) *J. Biol. Chem.* **247**, 1849-1860
22. Karu, A. E., MacKay, V., Goldmark, P. J., and Linn, S. (1973) *J. Biol. Chem.* **248**, 4874-4884
23. Taylor, A. F., and Smith, G. R. (1985) *J. Mol. Biol.* **185**, 431-443
24. Dixon, D. A., Churchill, J. J., and Kowalczykowski, S. C. (1994) *Proc. Natl. Acad. Sci. USA* **91**, 2980-2984
25. Roman, L. J., and Kowalczykowski, S. C. (1989) *Biochemistry* **28**, 2863-2873
26. Smith, G. R., Kunes, S. M., Schultz, D. W., Taylor, A., and Triman, K. L. (1981) *Cell* **24**, 429-436
27. Ponticelli, A. S., Schultz, D. W., Taylor, A. F., and Smith, G. R. (1985) *Cell* **41**, 145-151
28. Dixon, D. A., and Kowalczykowski, S. C. (1993) *Cell* **73**, 87-96
29. Julin, D. A., and Lehman, I. R. (1987) *J. Biol. Chem.* **262**, 9044-9051

30. Boehmer, P. E., and Emmerson, P. T. (1992) *J. Biol. Chem.* **267**, 4981-4987
31. Chen, H.-W., Randle, D. E., Gabbidon, M., and Julin, D. A. (1998) *J. Mol. Biol.* **278**, 89-104
32. Yu, M., Souaya, J., and Julin, D. A. (1998) *Proc. Natl. Acad. Sci. USA* **95**, 981-986
33. Wang, J., Chen, R., and Julin, D. A. (2000) *J. Biol. Chem.* **275**, 507-513
34. Zhang, X. J., and Julin, D. A. (1999) *Nucleic Acids Res.* **27**, 4200-4207
35. Chen, H.-W., Ruan, B., Yu, M., Wang, J., and Julin, D. A. (1997) *J. Biol. Chem.* **272**, 10072-10079
36. Taylor, A. F., and Smith, G. R. (2003) *Nature* **423**, 889-893
37. Dillingham, M. S., Spies, M., and Kowalczykowski, S. C. (2003) *Nature* **423**, 893-897
38. Singleton, M. R., Dillingham, M. S., Gaudier, M., Kowalczykowski, S. C., and Wigley, D. B. (2004) *Nature* **432**, 187-193
39. Rosamond, J., Telander, K. M., and Linn, S. (1979) *J. Biol. Chem.* **254**, 8646-8652
40. Taylor, A. F., and Smith, G. R. (1999) *Genes & Devel.* **13**, 890-900
41. Aggarwal, A. K. (1995) *Curr. Opin. Struct. Biol.* **5**, 11-19
42. Hlavaty, J. J., Benner, J. S., Hornstra, L. J., and Schildkraut, I. (2000) *Biochemistry* **39**, 3097-3105
43. Fenton, H. J. H. (1894) *J. Chem. Soc.* **65**, 899-110
44. Schepartz, A., and Cuenoud, B. (1990) *J. Am. Chem. Soc.* **112**, 3247-3249.
45. Hoyer, D., Cho, J., and Schultz, P. G. (1990) *J. Am. Chem.Soc.* **112**, 3249-3250.
46. Farber, J. M., and Levine, R. L. (1986) *J. Biol. Chem* **261**, 4574-4578.
47. Jens Lykke-Andersen1, R. A. G. a. J. K. (1997) *The EMBO Journal* **16**, 3272–3281
48. Schagger., H., and ., G. v. J. (1987) *Anal Biochem* **166**, 368-379
49. Zaychikov, E., Martin, E., Denissova, L., Kozlov, M., Markovtsov, V., Kashlev, M., Heumann, H., Nikiforov, V., Goldfarb, A., and Mustaev, A. (1996) *Science* **273**, 107-109
50. Wang, J., Chen, R., and Julin, D. A. (1999) *Anal. Biochem.* **273**, 310-313
51. Wang, J. (2000), University of Maryland
52. SE Tsutakawa, J., H. & Morikawa, K. (1999) *Cell* **99**, 615-623.
53. DB, S. M. a. W. (2002) *Journal of Bacteriology,* **Vol. 184**, 1819-1826,
54. Gill G, R.-R. A., Ghosh M, Burrows CJ, Rokita SE. (1997) *Chem Res Toxicol.* **10(3)**, 302-309
55. Stadtman ER. & Berlett, B. S. (1997) *Chem Res Toxicol* **10**, 485-494.